12-1979

Kinetic Study of the Formation of Mixed Ligand Complexes Formed from Triethylenetetramine Nickel (II) and Bidentate Ligands

Burtrand Insung Lee

KINETIC STUDY OF THE FORMATION OF MIXED LIGAND COMPLEXES FORMED FROM TRIETHYLENETETRAMINE NICKEL(II) AND BIDENTATE LIGANDS

by

Burtrand Insung Lee

A Thesis
Submitted to the
Faculty of The Graduate College
in partial fulfillment
of the
Degree of Master of Arts

Western Michigan University
Kalamazoo, Michigan
December, 1979

ACKNOWLEDGEMENTS

The completion of this thesis has been made possible through the advice and constructive criticism of Professor Ralph K. Steinhaus. My thanks go to him, as to the others at the Chemistry Department of Western Michigan University, who have not only shared their knowledge with me, but also their sense of scholarship and intellectual curiosity. The financial benefits and teaching experience have helped to make graduate study a pleasure and a privilege. It is not necessary to say that gratitude in any way divorces me from the sole responsibility for what is written here.

Burtrand Insung Lee

TABLE OF CONTENTS

CHAPTER PAGE

LIST OF TABLES

LIST OF TABLES (Continued)

LIST OF FIGURES

LIST OF FIGURES (Continued)

LIST OF FIGURES (Continued)

CHAPTER I

INTRODUCTION

The replacement of one ligand coordinated to a metal center by another free ligand in solution is a fundamental process which permeates all aspects of coordination chemistry. The substitution of a coordinated solvent molecule, usually water, by another complexing molecule is the basis of the formation of metal complexes.[1] This is exemplified by nickel(II) octahedral complex formation in equation 1 with k_f representing the second-order formation rate constant, where L is a multidentate ligand with i dentate sites.

$$Ni(H_2O)_6^{2+} + L \underset{}{\overset{k_f}{\rightleftharpoons}} Ni(H_2O)_{6-i}(L) + iH_2O \qquad (1)$$

Equation 1 shows that i molecules of water have to be lost before the ligand can form a complex with nickel(II). Therefore, the rate at which bound water is lost from nickel(II) is an important part of the reaction. It has been known that there is a relationship between the rate of water loss of the metal ion and the rate of formation of the complex. Rates of water loss from the metal ion in aqueous solution have been measured directly by a number of investigators using nuclear magnetic resonance methods[2-5] and have been calculated indirectly from substitution reactions by many others.[10-11]

In the normal substitution process, where the reaction rate is controlled by outer-sphere association between the metal ion and ligand and water loss of the metal ion, the formation rate can be estimated by eq. 2.

$$k_f = K_{os} k^{-H_2O} \quad (2)$$

Here, K_{os} is the outer-sphere association constant and k^{-H_2O} is the rate of water loss.[6] An expression for calculation of the outer-sphere association constant had originally been derived by Fuoss[7] and Eigen.[8]

The effect of coordinated ligands on the rate of replacement of the remaining water by ammonia in nickel(II) complexes has been investigated by Margerum and co-workers.[9-10] The rate of the water replacement is proportional to the number of aliphatic nitrogens co-ordinated to nickel(II), that is, the rate of water replacement is enhanced by the ligand already coordinated to the metal. Gordon and co-workers[11] have shown that an increase of water exchange rate is not necessarily seen as an increase in the rate of formation between the poly(ethyleneamine) nickel(II) complexes and aromatic bidentate ligands. They concluded by suggesting that there are factors other than water-exchange rate influencing the formation process. The need for more specific experiments to examine the other factors which influence the rates of formation is apparent and is the

basis of this study.

It is not difficult to see that the rates of formation can be accelerated by interactions in the outer-sphere or inhibited by steric effects. In multidentate ligands where initial bond formation is not the rate determining step (RDS), the rates of formation may be less than for the corresponding monodentate substitutions. Margerum et. al.[12] have suggested that the second coordinate bond formation contributes to the rate limiting value in the reaction between nickel(II) and bipyridyl. Jones and Margerum[13] have studied the kinetics between diaquobis(ethylenediamine) nickel(II) and ethylenediamine where pH dependence provides direct evidence for the contribution of ring closure to limiting rate in the chelation of the third ethylenediamine molecule. However, Cavasino and co-workers,[14-16] in their study of the formation of the nickel(II) complexes of alkyl- and benzyl malonic acid and phthalic acid, showed that there is little contribution of ring closure in RDS.

In the case of amino acids, which form six-membered rings, the mechanism for reaction of mono-complex formation between free Ni(II) and the amino acids, given by Kustin and Pasternack,[17-22] shows a slower than expected substitution process and has been termed

"sterically controlled substitution" (SCS). In other words, there are steric factors, which were not accounted for in the normal substitution reactions. Nonetheless, they have ignored the question whether the amino group or the carboxylate group bond first. Initial coordination of the amino group has been suggested by Wilkins;[6] however, Rorabacher[23] suggested and Margerum et. al.[24] have discussed in detail why the carboxylate group bonds first followed by a slower ring closure of the amino group. They suggest that this pertains to both five- and six-membered rings. However, it is not improbable that ligands already coordinated to the metal may slow the rate considerably.

Steric effects in chelation kinetics between nickel(II) and N-alkyl derivatives of ethylenediamine have been noted in studies of Rorabacher[25] and Turan.[26] Here again, the location of RDS is believed to shift from first-bond formation with en to second-bond formation with highly substituted diamines; whereas, severely hindered reactants do not form a complex.

In this study, the formation reactions between tetra-chelated nickel(II) complex with triethylenetetramine and a number of bidentate ligands in aqueous medium are studied. The position of RDS, steric effects, and the effect of coordinated triethylenetetramine are to be examined.

CHAPTER II

APPARATUS AND REAGENTS

Apparatus

All spectra and absorbance values of reactants and products were obtained on a Cary Model 14 spectrophotometer with various length of cells. In most cases, the instrument was operated at maximum slit height and automatic slit width with slit control at 25 and dynode tap at 2.

All kinetic measurements were made on an Aminco-Morrow Stopped-Flow Apparatus attached to a Shimadzu QV-50 Spectrophotometer. The spectral changes from the latter were displayed on a Tektronix 5103N storage oscilloscope and stored in a Biomation Waveform Recorder Model 805. The displays were recorded on Polaroid film and/or a Sargent Recorder Model SR using the Biomation stored data. Constant temperature was maintained by running water through the reactants reservoir site of the stopped-flow compartment.

All pH measurements were made on a Beckman Research Model pH meter using a saturated calomel reference electrode which was filled with a saturated solution of sodium chloride.

Reagents

All solutions were prepared from reagent grade chemicals, unless otherwise specified, using distilled water that had been purified through a deionizing column of Amberlite MB-3 mixed bed resin.

Standard copper(II) nitrate

Heavy foil copper (99.96% pure), manufactured by J. T. Baker Chemical Co., was washed with dilute nitric acid, water and ethanol. After drying, it was weighed and dissolved in a minimum amount of concentrated nitric acid and diluted to volume.

Ethylenediaminetetraacetic acid

Aldrich Chemical Analyzed reagent grade dihydrated disodium salt was used without further purification. It was standardized[27] with standard copper(II) nitrate solution using naphthylazoxin S. (NAS) (0.1 M) as an indicator. pH was maintained at 5.5 by an acetate buffer.

Acetate buffer

Sodium acetate ($NaC_2H_3O_2 \cdot 3H_2O$) was dissolved in water which contained hydrochloric acid to make up a buffer of pH 5.5.

Nickel(II) nitrate

A tenth molar solution was prepared from nickel nitrate hexahydrate reagent. The solution was standardized[27] at pH 5.5 by titration with EDTA using NAS as the indicator.

Triethylenetetramine

Triethylenetetramine disulfate ($C_6H_{18}N_4.2H_2SO_4$) from J. T. Baker was recrystallized twice from hot water and methanol. A tenth molar solution was prepared.

Triethylenetetraminenickel(II)[28]

A slight molar excess of nickel(II) nitrate solution was added to a triethylenetetramine(trien) solution and the pH was raised to 11.5 by adding sodium hydroxide to precipitate the excess nickel as nickel(II) hydroxide. The precipitate was filtered out on a 0.45μ Millipore filter with vacuum suction until the $Ni(trien)^{2+}$ solution became clear. The pH was brought down to 9 by adding sulfuric acid. The $Ni(trien)^{2+}$ solution was dark blue in color and was standardized by adding a 100-fold excess of sodium cyanide to give tetracyanonickelate(II) and comparing the absorbance at wavelength 267 nm with a standard $Ni(CN)_4^{2-}$ solution.

The concentration of $Ni(trien)^{2+}$ solution was checked by a mole-ratio plot. The mole-ratio plot was prepared using data obtained by adding excess Cu^{2+} to varying amounts of $Ni(trien)^{2+}$. The molar absorptivity ($\in$) of $Cu(trien)^{2+}$ was obtained from a mole-ratio plot prepared by using data obtained by adding excess trien to varying amounts of standard Cu^{2+}. The absorbance values were taken at 550 nm with the slit control at 10. The pH was held constant at 5 by acetate buffer. The concentration of $Ni(trien)^{2+}$, determined from $Ni(CN)_4^{2-}$ and from the mole-ratio plot, agreed within 0.15%.

Borate buffer

An equimolar mixture of boric acid and sodium tetraborate ($Na_2B_4O_7 \cdot 10H_20$) with varying amounts of mannitol yielded a series of buffers with a pH ranging from 4.7 to 9. Buffers of pH above 9 were prepared by adding sodium hydroxide to the original buffer.

Sodium Choloride (1 M)

Reagent grade sodium chloride was dissolved in water and diluted to volume.

1,10-Phenanthroline (0.015 M)

G. F. Smith reagent grade white colored

1,10-phenanthroline monohydrate ($C_{12}H_8N_2:H_2O$) was dissolved in hot water and diluted to volume. The concentration of the solution was close to the maximum solubility in water. The pH of the solution was measured to be 7.85.

2,2'-Bipyridyl (0.015 M)

Matheson Coleman & Bell reagent grade 2,2'-bipyridyl was dissolved in hot water and diluted to volume.

Ethylenediamine Dihydrochloride (0.50 M)

Approximately 100 ml of Matheson Coleman & Bell reagent grade ethylenediamine (en) (99% pure) were dehydrated with 15g of sodium hydroxide pellets on a steam bath by refluxing for 10 hours. The dehydrated en was distilled at 116°C. The distilled en was stored in a brown bottle under nitrogen. It was crystallized by bubbling through anhydrous hydrogen chloride gas for 20 minutes in 150 ml of absolute ethyl alcohol. The product (1,2-diaminoethane hydrochloride) was washed with absolute ethanol and dried in an oven at 105°C for 2 hours before being placed in a vacuum desiccator. The salt was dissolved in water and the pH of the resulting solution was 5.25.

n-Propyl amine

Approximately 250 ml of Eastman Kodak reagent grade n-propyl amine was dehydrated by adding 150g of sodium hydroxide pellets to the liquid and heating on a steam bath for 3 hours and distilled at 47.8°C. The liquid was crystallized as was done with en to produce white-colored n-propyl amine hydrochloride. A two-tenth molar solution was prepared.

7,8-Benzoquinoline

Aldrich reagent grade 7,8-Benzoquinoline (ben) (97% pure; brownish-yellow in color) was recrystallized from an ethanol water mixture twice. The recrystallized benzoquinoline was light yellow in color. Since this was insoluble in water, both a 50% by volume water-dioxane mixture and a 60% by volume methanol-water mixture were used to make up 0.020 M solution.

2-Phenyl pyridine (0.020 M)

Aldrich reagent grade 2-phenyl pyridine (phpy) (98% pure; brownish yellow in color) was distilled under vacuum at 105°C. The distilling flask was placed in an oil bath and stirred. The distilled phpy was light yellow in color and stored in the original brown bottle.

Solutions were prepared in both a 50% by volume

dioxane-water mixed solvent and a 60% by volume methanol-water mixed solvent.

Glycine

Aldrich reagent grade glycine (98%) was recrystallized from water and methanol. It was white in color. A five-tenth molar solution was prepared.

2-Pyridinecarboxylic acid

J. T. Baker practical grade picolinic acid was recrystallized three times from methanol and petroleum ether. The melting point of the recrystallized acid was 136-137°C which compared to a literature value of 136-7°C. A four-tenth molar solution was prepared.

TABLE I

List of Abbreviations and Symbols

Ethylenediaminetetraacetic acid	EDTA
Triethylenetetramine	trien; T
Diethylenetriamine	dien
2,2',2"-Triaminotriethylamine	tren
1,10-Phenanthroline	phen; P
2,2'-Bipyridyl	bipy
n-Propylamine	$prNH_2$
Ethylenediamine	en
7,8-Benzoquinoline	ben
2-Phenylpyridine	phpy
Glycine	gly
2-Pyridinecarboxylic acid	pyc
Napthyl Azoxin S.	NAS
Rate Determining Step	RDS
Internal Conjugate Base	ICB
Sterically Controlled Substitution	SCS
Molar Absorptivity	$\in$
Absorbance	Abs; A
Cell Path Length	b
Concentration	C
Ionic Strength	μ
Wavelength	λ
Time	t

CHAPTER III

EXPERIMENTAL

The ionic strength of all reactant solutions was maintained at 0.1 M with NaCl. The desired pH was obtained using a borate-mannitol buffer. All spectrophotometric studies were done at room temperature. All kinetic runs were done in triplicate and the mean values are used. The temperature was kept at $25 \pm 0.5^{\circ}C$ by means of a circulating water bath. With the slit completely closed, the stopped-flow apparatus was set at zero percent transmittance. Deionized water was placed in the mixing chamber of the apparatus, the slit was opened and one hundred precent transmittance was set. Experimental conditions used for each ligand are listed in Table 2.

Triethylenetetramine Nickel(II) And 1,10-Phenanthroline

Spectrophotometric study

$Ni(trien)^{2+}$ and phen were each diluted from stock solutions to give two solutions of 7.56×10^{-4} M in concentration at pH 8.7. A $Ni(trien)(phen)^{2+}$ solution was prepared according to eq. 3

$$Ni(trien)^{2+} + phen \rightleftharpoons Ni(trien(phen)^{2+} \qquad (3)$$

by mixing equimolar solutions of $Ni(trien)^{2+}$ and phen to give a concentration of 7.56×10^{-4} M at pH 8.7

TABLE 2

Ligands and Experimental Conditions Used in the Study[a]

Ligand	pK_a[b]	pH range	λ,nm	Range of $[Ni(trien)^{2+}]x10^3$,M	Range of $[L]x10^3$,M
7,8-Benzoquinoline	3.1[c]	4 - 5		d	d
2,2'-Bipyridyl	4.42,1.5	8 - 9	305	0.05	0.5-1.5
Ethylenediamine[e]	10.1,7.3	10-11	260	2-10	20-80
Glycine	9.57,2.36	4 - 9	260	3.1-6.0	6.0-1.60
1,10-phenanthroline	4.93,1.9	8.2-8.8	343	0.075-1.5	0.75-2.25
2-phenylpyridine	3.9[c]	4 - 5		d	d
n-propylamine[e]	10.74	10-11	270	8	8-20
2-pyridinecarboxylic acid	5.21,1.03	4 - 9	243	0.0151-0.0237	0.151-0.711

a. Ionic strength, μ = 0.1 M, temperature 25 + 0.5°C
b. Cited from A. E. Martell and R. M. Smith, "Critical Stability Constant," 1974
c. Estimated in 60% v/v methanol-water in this study
d. No kinetic measurements taken because no reaction occurred
e. Kinetics was complicated, a simple formation reaction could not be resolved

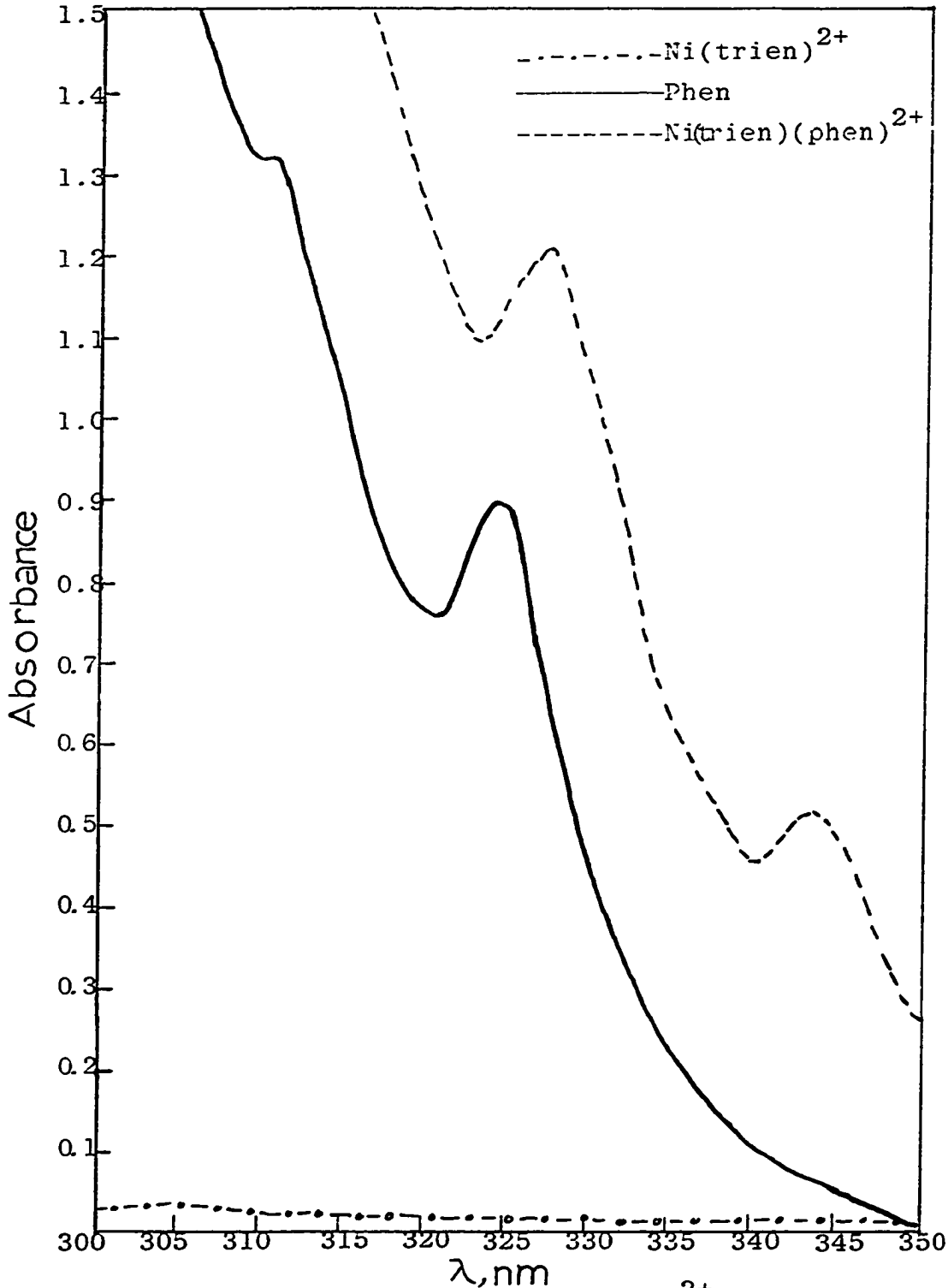

Figure 1. U. V. Spectra of $Ni(trien)^{2+}$, Phen, and Ni(trien)(phen), b = 2 cm, C = 7.56 x 10^{-4}M, pH = 8.7

TABLE 3

Spectral Data of $Ni(trien)^{2+}$, Phen and $Ni(trien)(phen)^{2+}$ at 343 nm, μ = 0.1 M, Concentration = 7.56×10^{-4} M and pH = 8.7

Solution	Cell Path, cm	Abs.	ϵ	$\Delta\epsilon$
$Ni(trien)^{2+}$	10	0.068	8.8	
Phen	2	0.071	47	291
$Ni(trien)(phen)^{2+}$	2	0.510	338	

Absorption spectra of these three solutions were obtained in the region of 300-350 nm at room temperature. The spectra are shown in Fig. 1. Table 3 lists the absorbances and molar absorptivities found at λ = 234 nm, the wavelength showing the greatest difference in molar absorptivity ($\Delta\epsilon$) between the reactants and the product. This wavelength was chosen to follow the kinetics of the reaction between $Ni(trien)^{2+}$ and phen.

Kinetics of the reaction

Pseudo first-order runs

A 1.50×10^{-4} M $Ni(trien)^{2+}$ solution at μ = 0.1 M was prepared and adjusted to pH 8.7. Ten-, twenty-, and thirty-fold excess phen solutions relative to $Ni(trien)^{2+}$ were prepared at μ = 0.1 M and adjusted to pH 8.7. The reactant solutions were mixed in the stopped-flow spectrophotometer and the transmittance changes, shown on the oscilloscope screen, were recorded on a Polaroid film. The percent transmittance values were taken from the photographs.

Second-order runs

Three sets of $Ni(trien)^{2+}$ and phen, all at the same concentration, 3.0×10^{-3} M, but at pH values ranging from 8.2 to 8.8 were prepared. The recording of the

transmittance changes were carried out as described above. The pH of the mixed solutions were measured by mixing equal volumes of each reactant for each set.

Triethylenetetramine Nickel(II) And 2,2'-Bipyridyl

Spectrophotometric study

$Ni(trien)^{2+}$ and bipy were each diluted from stock solutions to give two solutions of 3.71×10^{-5} M in concentration at pH 7.8. A $Ni(trien)(bipy)^{2+}$ solution was prepared according to eq. 4 by mixing equimolar solutions of $Ni(trien)^{2+}$ and bipy to give 3.71×10^{-5} M at pH 7.8. Absorption spectra of these three solutions

$$Ni(trien)^{2+} + bipy \rightleftharpoons Ni(trien)(bipy)^{2+} \quad (4)$$

were obtained in the region of 280-330 nm and are shown in Fig. 2.

Since the absorption of $Ni(trien)^{2+}$ at the concentration was negligible, only bipy and $Ni(trien)(bipy)^{2+}$ are shown. It is seen from Fig. 2 that a wavelength of 305 nm gives a large molar absorptivity difference between $Ni(trien)(bipy)^{2+}$ and bipy. The values of absorbance, molar absorptivity and the difference in molar absorptivity between $Ni(trien)(bipy)^{2+}$ and bipy are listed in Table 4.

Kinetics of the reactions

Second-order runs were not necessary because of the large spectral change for the reaction with low noise at $\lambda = 305$ nm.

A 1.0×10^{-4} M of $Ni(trien)^{2+}$ solution, $\mu = 0.1$ M was adjusted to pH 8.9. Ten-, twenty-, and thirty-fold excess bipy solutions relative to $Ni(trien)^{2+}$ were prepared at $\mu = 0.1$ M and adjusted to pH 8.7. The solutions were mixed in the stopped-flow spectrophotometer, the spectral changes were stored in the Biomation transient recorder and read out on a Sargent Recorder Model SR as well as recorded on Polaroid film from the oscilloscope screen.

Triethylenetetramine Nickel(II) And Ethylenediamine

Titration of ethylenediamine hydrochloride salt solution

A 50.0 ml of 0.050 M ethylenediamine hydrochloride salt solution was titrated potentiometrically using a Beckman Research Model pH meter with carbonate-free standard NaOH, 0.09414 M, which had been standardized with potassium acid phthalate primary standard using phenolphthalein as the indicator. The titration plot of pH vs volume of NaOH gives two points of inflection as shown in Fig. 3.

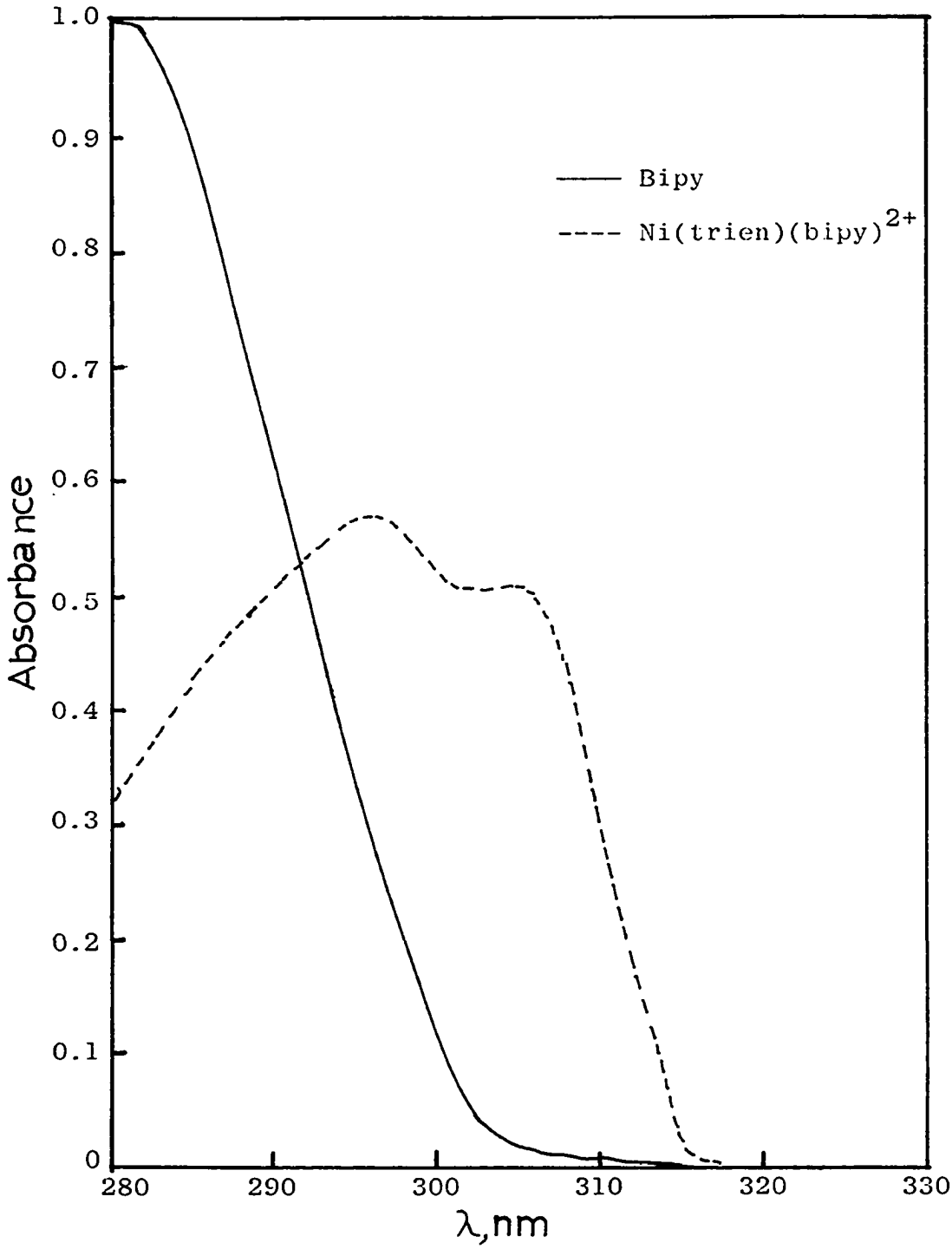

Figure 2. U. V. Spectra of Bipy and $Ni(trien)(bipy)^{2+}$, b = 2 cm, C = 3.71 x 10^{-5} M, pH = 7.8

TABLE 4

Spectral Data of Bipy and Ni(trien)(bipy)$^{2+}$
At λ = 305 nm, μ = 0.1 M, 3.71 x 10^{-5} M and at pH 7.8

Solution	Cell Path, cm	Abs.	$\in$ x 10^{-2}	$\in$ x 10^{-2}
bipy	2	0.01	1.35	67.4
Ni(trien)(bipy)$^{2+}$	2	0.51	68.7	

Spectrophotometric study

The ethylenediamine stock solution was diluted to 1.0×10^{-2} M at pH 8.9. A solution of $Ni(trien)(en)^{2+}$ was prepared according to eq. 5 by mixing equimolar

$$Ni(trien)^{2+} + en \rightleftharpoons Ni(trien)(en)^{2+} \quad (5)$$

volumes of $Ni(trien)^{2+}$ and en stock solutions to give a solution with a concentration of 5.0×10^{-3} M at pH 10.9. The absorption spectra were obtained from these solutions and are shown in Fig. 4. The absorption of en was negligible and not shown. A wavelength of 260 nm was used to run kinetics although several other wavelengths were tried. A study of absorbance with pH change of $Ni(trien)^{2+}$ and $Ni(trien)(en)^{2+}$ was done at 300 nm. No significant changes in absorbance were seen as pH increased. The absorbance data are given in Table 5 and the spectral data at 260 nm are listed in Table 6.

Kinetics of the reaction

Pseudo first-order runs

Stock solutions of $Ni(trien)^{2+}$ and en were diluted to 1.0×10^{-2} M and 1.0×10^{-1} M respectively at pH 10.2 and $\mu = 0.1$ M. Using the stopped-flow spectrophotometer, the normal spectral changes for the reaction were not observed at the highest sensitivity and fastest sweep time allowed by noise.

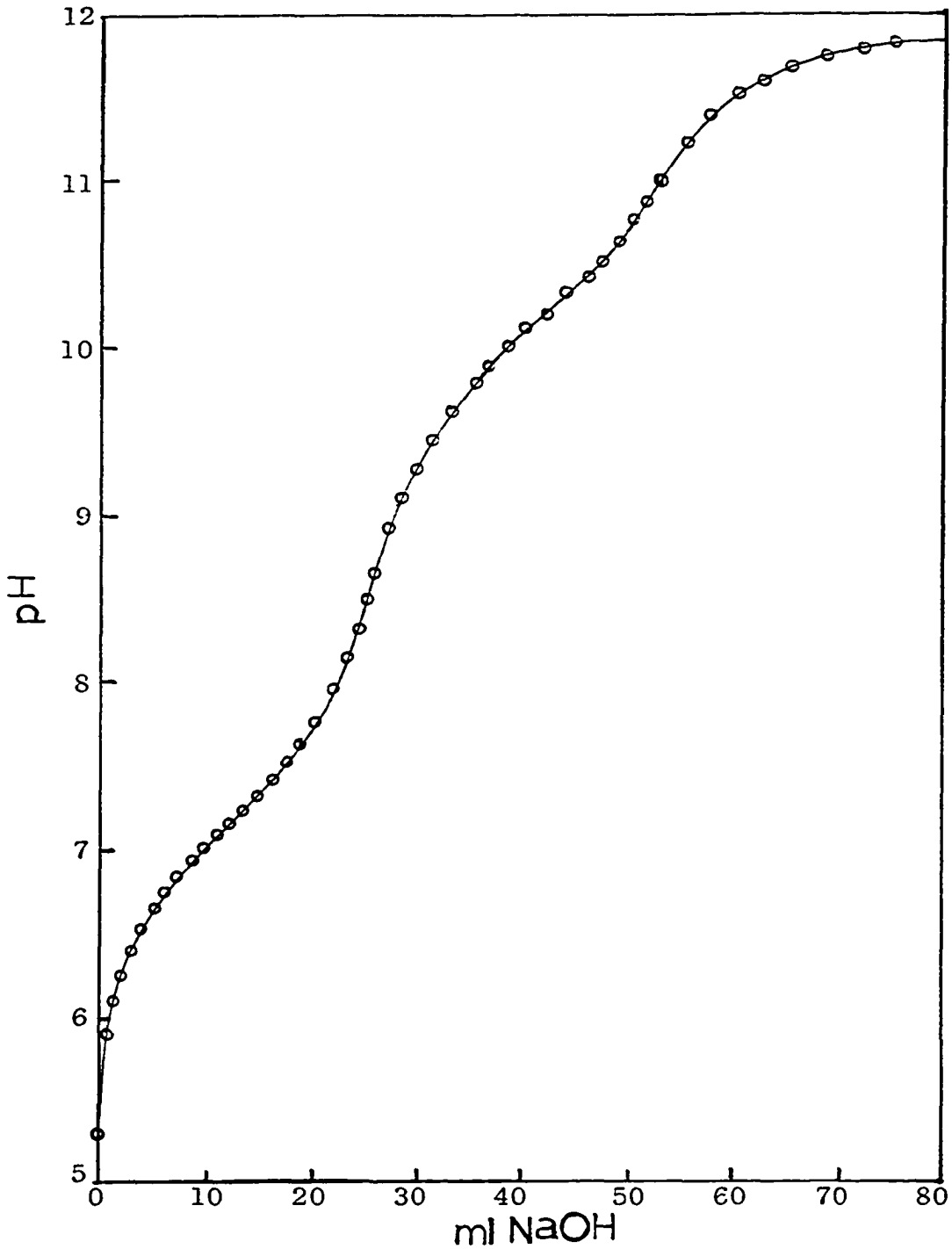

Figure 3. Potentiometric titration plot of Ethylenediamine Hydrochloride salt [NaOH] = 0.09414 M, [en · nHCl] = 0.050 M.

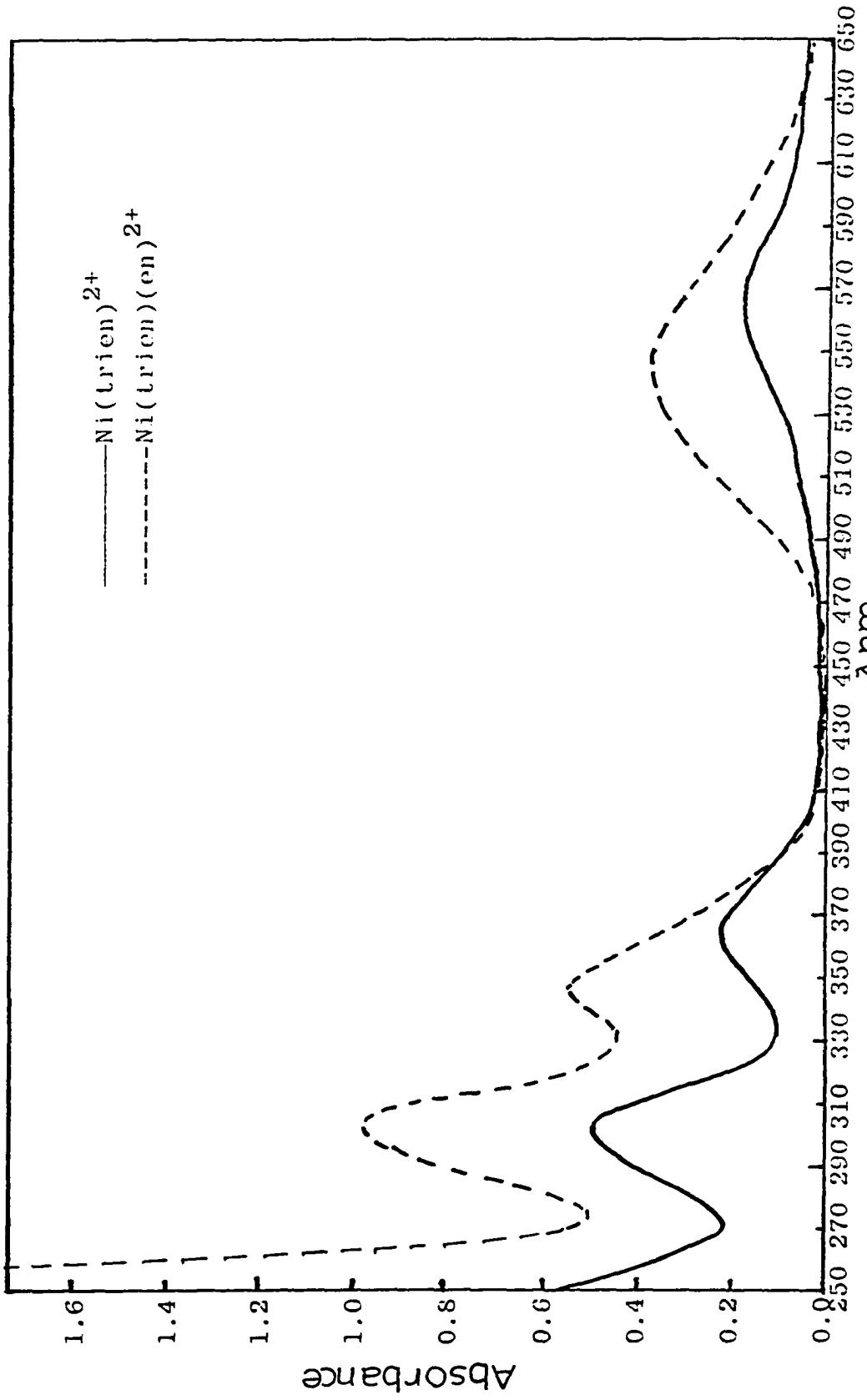

Figure 4. U. V. and visible spectra of Ni(trien)$^{2+}$ and Ni(trien)(en)$^{2+}$, b = 5 cm, C = 5.0 x 10^{-3} M, pH = 10.9

Second-order runs

A set of $Ni(trien)^{2+}$ and en solutions, 1.0×10^{-2} M at pH 10.9 and μ = 0.1 M were used. No spectral changes for the reaction were observed on the stopped-flow spectrophotometer at the highest sensitivity and fastest sweep time allowed by noise.

Triethylenetetramine Nickel(II) And n-Propylamine

Spectrophotometric study

Stock solutions of $Ni(trien)^{2+}$ and $prNH_2$ were diluted to 8.0×10^{-3} M. Equimolar volumes of the two stock solutions were mixed according to eq. 6 to prepare 8.0×10^{-3} M $Ni(trien)(prNH_2)^{2+}$. Absorption spectra

$$Ni(trien)^{2+} + prNH_2 \rightleftharpoons Ni(trien)(prNH_2) \qquad (6)$$

were obtained from the three solutions and are shown in Fig. 5. Since $prNH_2$ gave no detectable absorption at the concentration, only $Ni(trien)^{2+}$ and $Ni(trien)(prNH_2)^{2+}$ are shown. The largest change in molar absorptivity between $Ni(trien)^{2+}$ and $Ni(trien)(prNH_2)^{2+}$ occurred at 270 nm. The spectral data at that wavelength are listed in Table 7 and kinetic runs were carried out at that wavelength.

Kinetics of the reaction

Since the $\Delta\epsilon$ between the reactants and product at

TABLE 5

Absorbance Values of $Ni(trien)^{2+}$ and $Ni(trien)(en)^{2+}$ at Various pH's and λ = 300 nm

$Ni(trien)^{2+}$, 4.0×10^{-3} M b = 5 cm		$Ni(trien)(en)^{2+}$, 2.0×10^{-3}M b = 10 cm	
pH	Abs	pH	Abs
7.6	0.382	7.50	0.478
8.0	0.393	7.96	0.455
8.7	0.369	8.40	0.449
9.4	0.393	8.50	0.405
10.0	0.389	9.60	0.412
10.4	0.393	10.20	0.434
11.2	0.419	10.50	0.412
		10.80	0.389

TABLE 6

Spectral Data of En, $Ni(trien)^{2+}$ and $Ni(trien)(en)^{2+}$
At λ = 260 nm, μ = 0.1 M, 5.0 x 10^{-3} M and pH 10.9

Solution	Cell Path, cm	Abs.	ϵ	$\Delta\epsilon$
en	10	0.00	0	
$Ni(trien)^{2+}$	10	0.49	10	49
$Ni(trien)(en)^{2+}$	5	1.47	59	

λ = 270 nm is so small (3.3), and the absorbance of $prNH_2$ at higher concentration is not negligible, pseudo first-order runs could not be made. The second-order runs were attempted at pH 10 using 2.66 x 10^{-2} M solutions of $Ni(trien)^{2+}$ and $prNH_2$. No detectable transmittance changes were observed on the stopped-flow spectrophotometer at the highest sensitivity and fastest sweep time allowed by noise.

Triethylenetetramine Nickel(II) and 7,8-Benzoquinoline in 50% Dioxane by Volume

Estimation of pK_a value of Benzoquinoline

Two solutions of benzoquinoline at pH 2 and 9, both of equal concentration in 50% v/v dioxane-water, were prepared. Absorption spectra were obtained and are shown in Fig. 6. Then the absorbance values of solutions in 50% v/v dioxane-water, at pH's ranging from 1.0 to 10.0, were obtained at λ = 360 nm. A plot of absorbance vs pH was made and is shown in Fig. 7. The pK_a value of benzoquinoline was estimated, from the inflection point of the curve, as 2.7.

Spectrophotometric study

Benzoquinoline stock solution was diluted to 1.0 x 10^{-4} M and 1.0 x 10^{-5} M with 50% v/v dioxane-water.

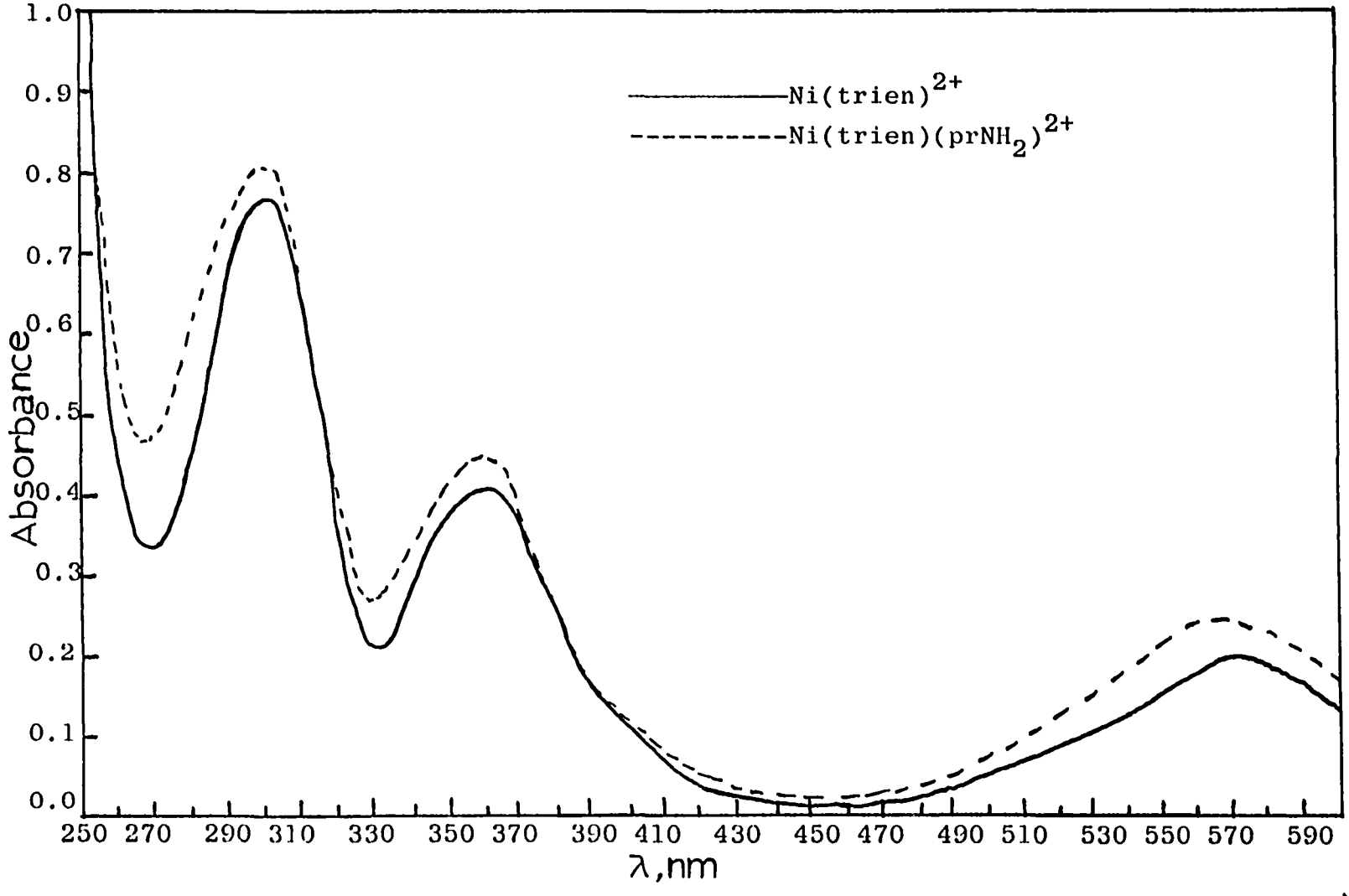

Figure 5. U. V. and visible spectra of $Ni(trien)^{2+}$ and $Ni(trien)(prNH_2)^{2+}$, b = 5 cm, C = 8.0×10^{-3} M and pH = 10.0

TABLE 7

Spectral Data of $prNH_2$, $Ni(trien)^{2+}$ and $Ni(trien)(prNH_2)^{2+}$ At λ = 270 nm, μ = 0.1 M, C = 8.0×10^{-3} M and at pH 10.0

Solution	Cell Path, cm	Abs.	ϵ	$\Delta\epsilon$
$prNH_2$	5	0.0	0.0	
$Ni(trien)^{2+}$	5	0.34	8.5	3.3
$Ni(trien)(prNH_2)^{2+}$	5	0.47	11.8	

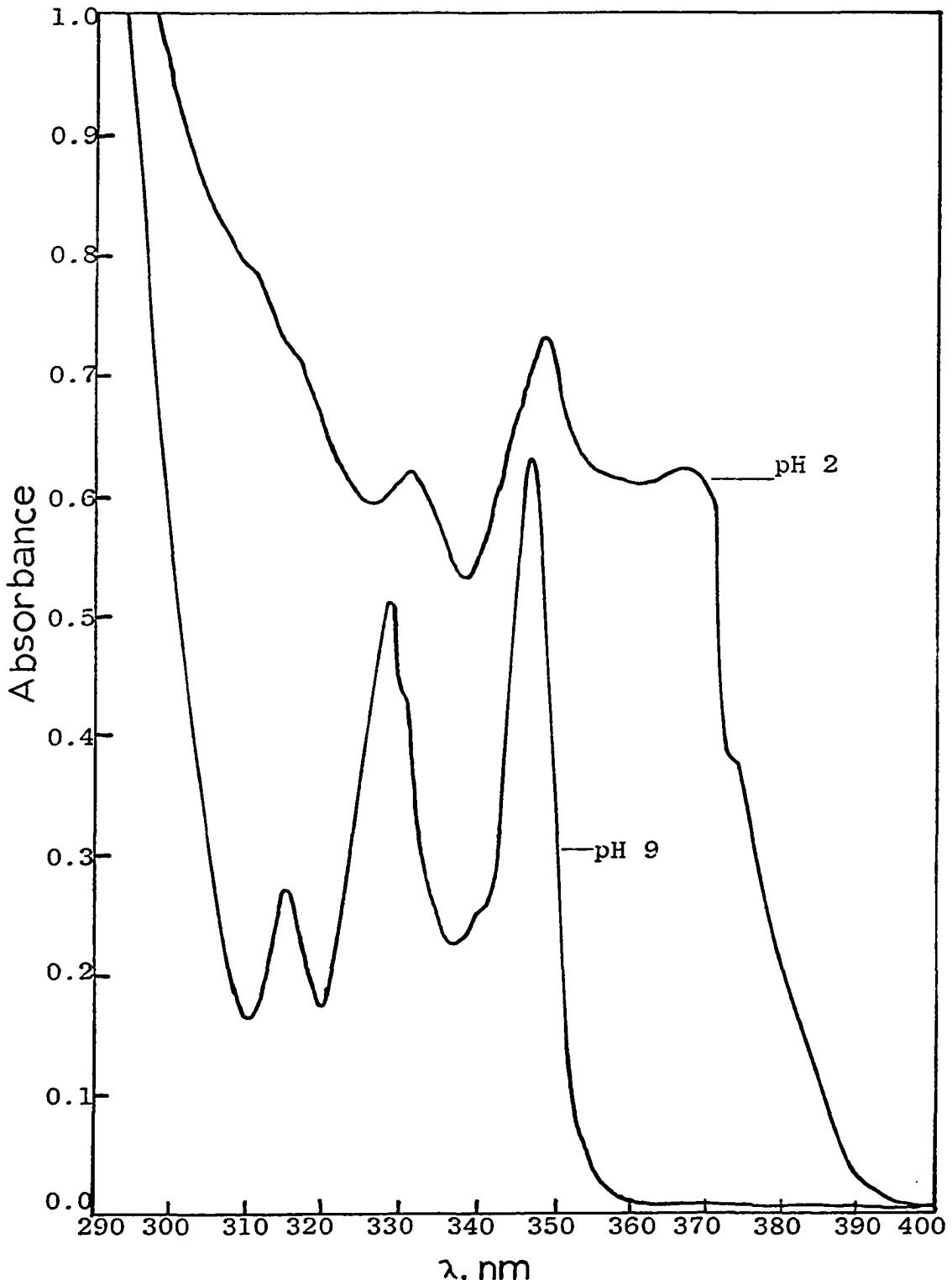

Figure 6. U. V. Spectra of Benzoquinoline at pH 2 and 9 in 50% v/v Dioxane, b = 2 cm, C = 1.0 x 10^{-4} M

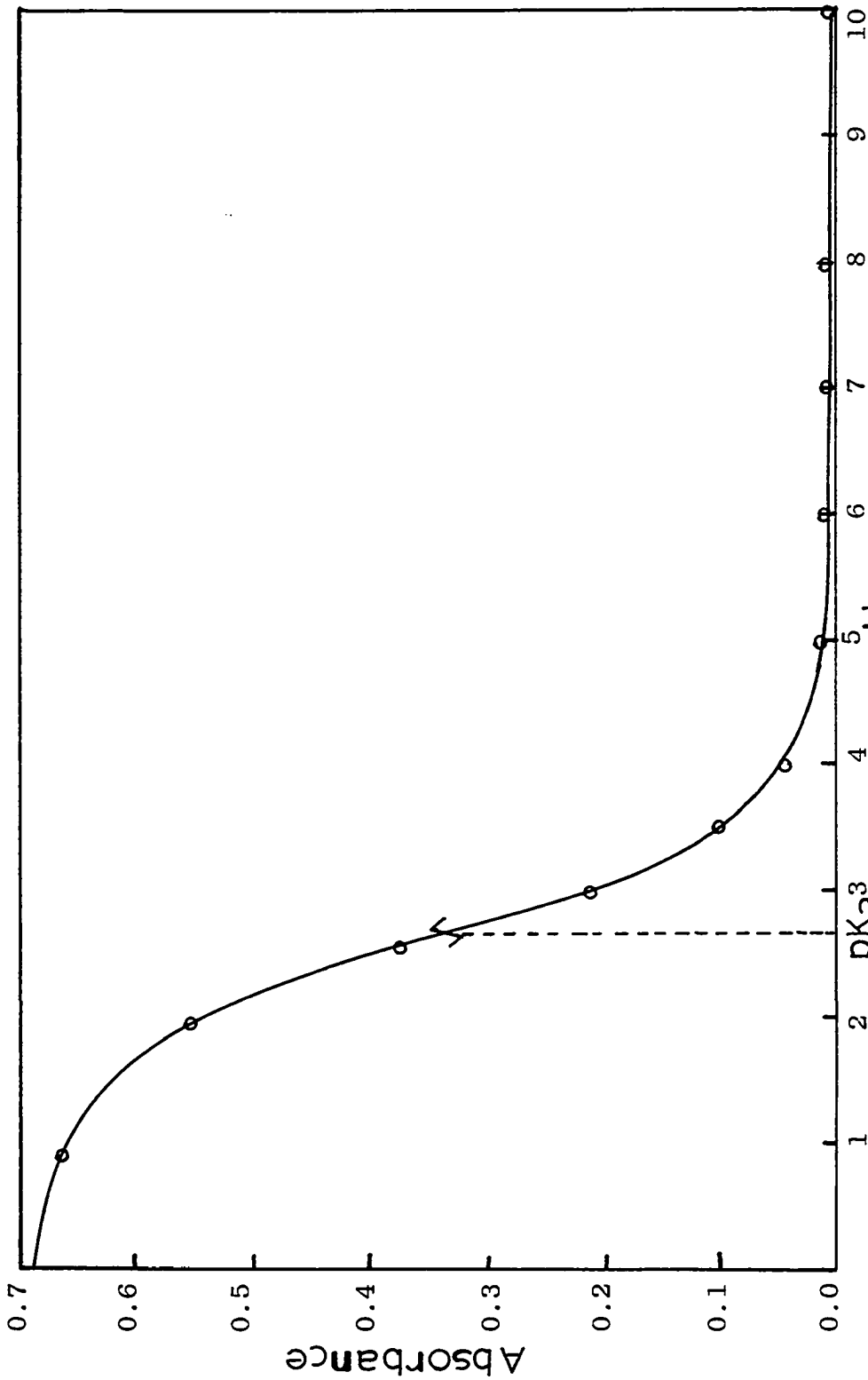

Figure 7. Estimation of pK_a value of 7,8-Benzoquinoline in 50% v/v Dioxane
λ = 360, C = 2 x 10^{-4} M, b = 1 cm

$Ni(trien)^{2+}$ stock solution was diluted to 5.0×10^{-3} M with the 50% v/v dioxane. Equimolar volumes of $Ni(trien)^{2+}$ and ben were mixed together according to eq. 7 to give a solution of 5.0×10^{-3} M in concentration.

$$Ni(trien)^{2+} + ben \rightleftharpoons Ni(trien)(ben)^{2+} \qquad (7)$$

Absorption spectra of the three solutions were obtained right after the solutions were prepared and again the next day. The diluted $Ni(trien)^{2+}$ solution, 5.0×10^{-3} M appeared to be slightly bluish in color at the time of preparation but after 3 days, the color disappeared. This may have been due to a solvolysis reaction between $Ni(trien)^{2+}$ and dioxane (or dioxane-water). The absorption spectra are shown in Fig. 8. The spectra showed that $Ni(trien)^{2+}$ and ben in 50% dioxane-water do not react under the experimental conditions and as in eq. 7. Rather there appears to be a solvent interaction.

Triethylenetetramine Nickel(II) and 7,8-Benzoquinoline in 60% v/v Methanol-Water

The same studies as described above were carried out in 60% v/v methanol-water. The pK_a value was estimated to be 3.1. The absorption spectra of benzoquinoline, and $Ni(trien)^{2+}$ plus ben, both in 60% methanol-water, showed that there again was no formation reaction that takes place between $Ni(trien)^{2+}$ and ben as written in eq. 7. Figure 9 gives the spectra.

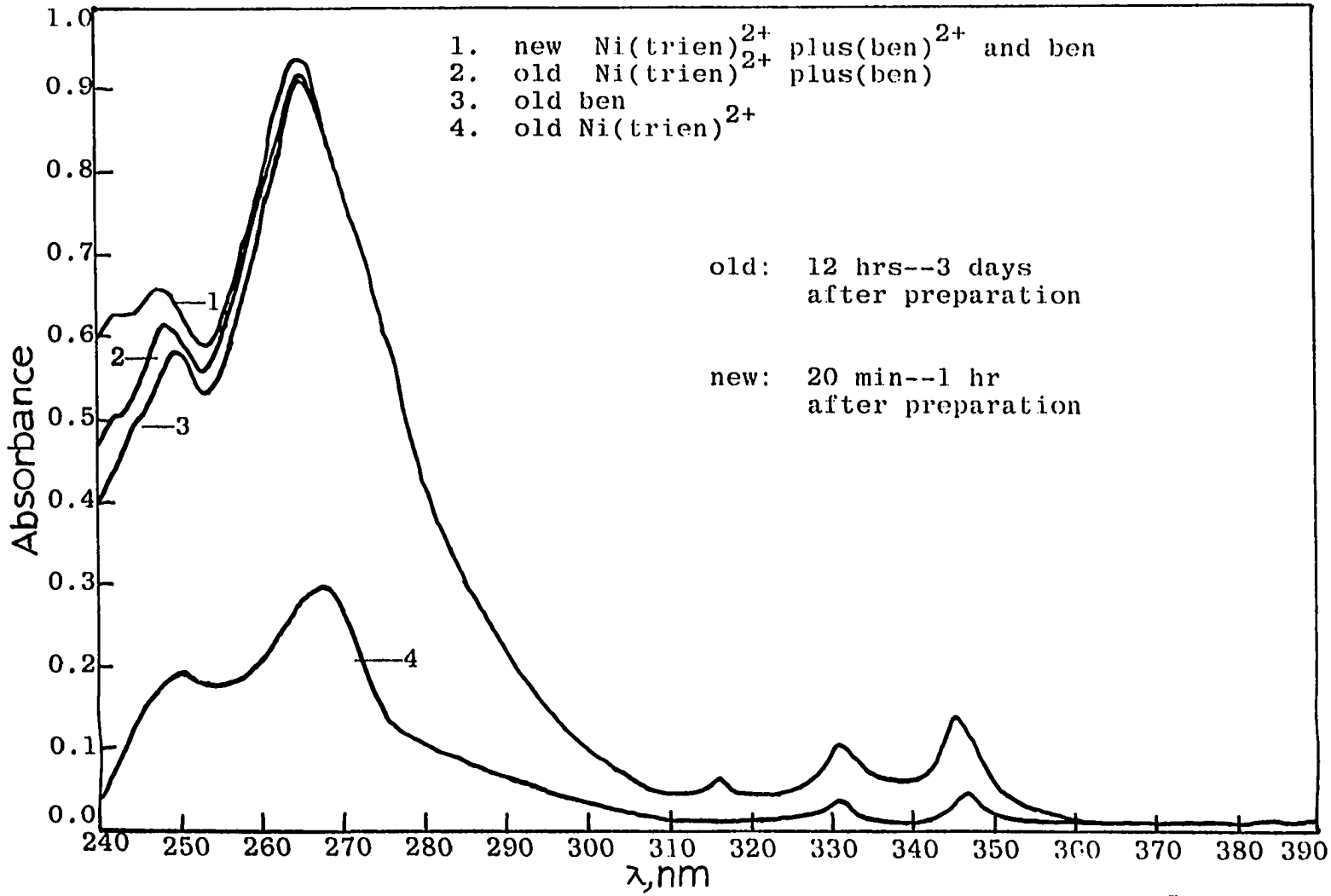

Figure 8. U. V. Spectra of Old and New Ni(trien)(ben)$^{2+}$, Ni(trien)$^{2+}$ and ben in 50% v/v Dioxane, C = 2.0 x 10^{-5} M, b = 2 cm, μ = 0.1 M and pH = 9

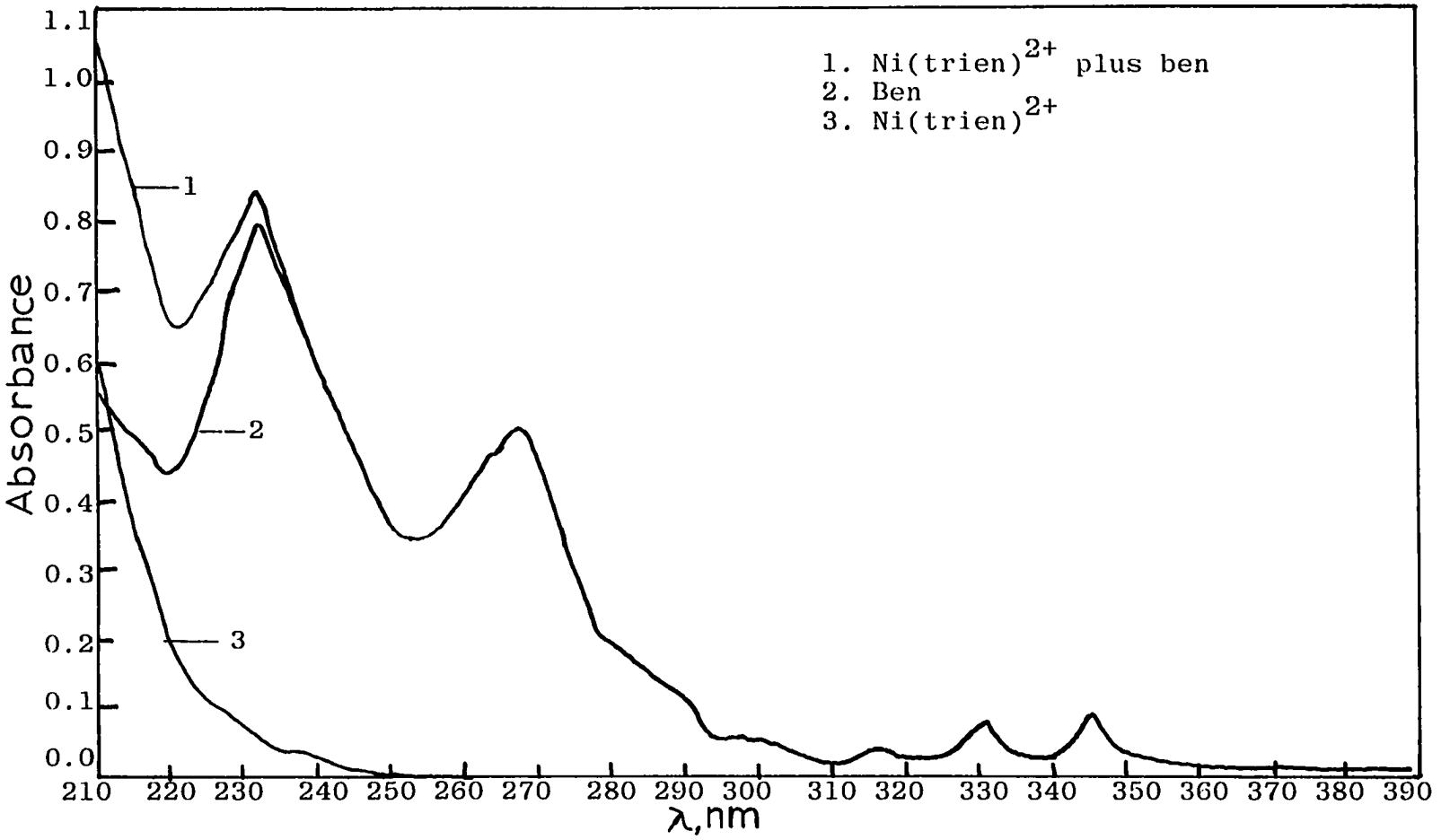

Figure 9. U. V. Spectra of $Ni(trien)^{2+}$, ben, and $Ni(trien)^{2+}$ plus ben in 60% v/v Methanol-water, b = 1 cm, C = 2 x 10^{-5} M and μ = 0.1 M

Triethylenetetramine Nickel(II) And 2-Phenylpyridine in 50% v/v Dioxane-Water and 60% v/v Methanol-Water

The same experiments as described above were carried out using 2-phenylpyridine in place of benzoquinoline in both 50% v/v/ dioxane-water and 60% v/v methanol-water. The pK_a value in 60% v/v methanol-water was estimated to be 3.8 but not measured in 50% v/v dioxane-water. The spectra of $Ni(trien)^{2+}$, phpy, and $Ni(trien)^{2+}$ plus phpy in 60% v/v methanol-water at pH 8.7 are shown in Fig. 10. It appears from the spectra that no reaction had occurred between $Ni(trien)^{2+}$ and phpy under the experimental conditions and as written in eq. 7.

Triethylenetetramine Nickel(II) and Glycine

Spectrophotometric study

Glycine and $Ni(trien)^{2+}$ stock solutions were diluted to 2.0×10^{-3} M at pH 9.8. $Ni(trien)(gly)^{+}$ was prepared according to eq. 8 by mixing equimolar

$$Ni(trien)^{2+} + gly^{-} \rightleftharpoons Ni(trien)(gly)^{+} \qquad (8)$$

volumes of $Ni(trien)^{2+}$ and glycine to give $Ni(trien)(gly)^{+}$ solution with a concentration of 2.0×10^{-3} M at pH 9.7. The resulting solution gave a light pink in color. The absorption spectra of these three solutions were obtained

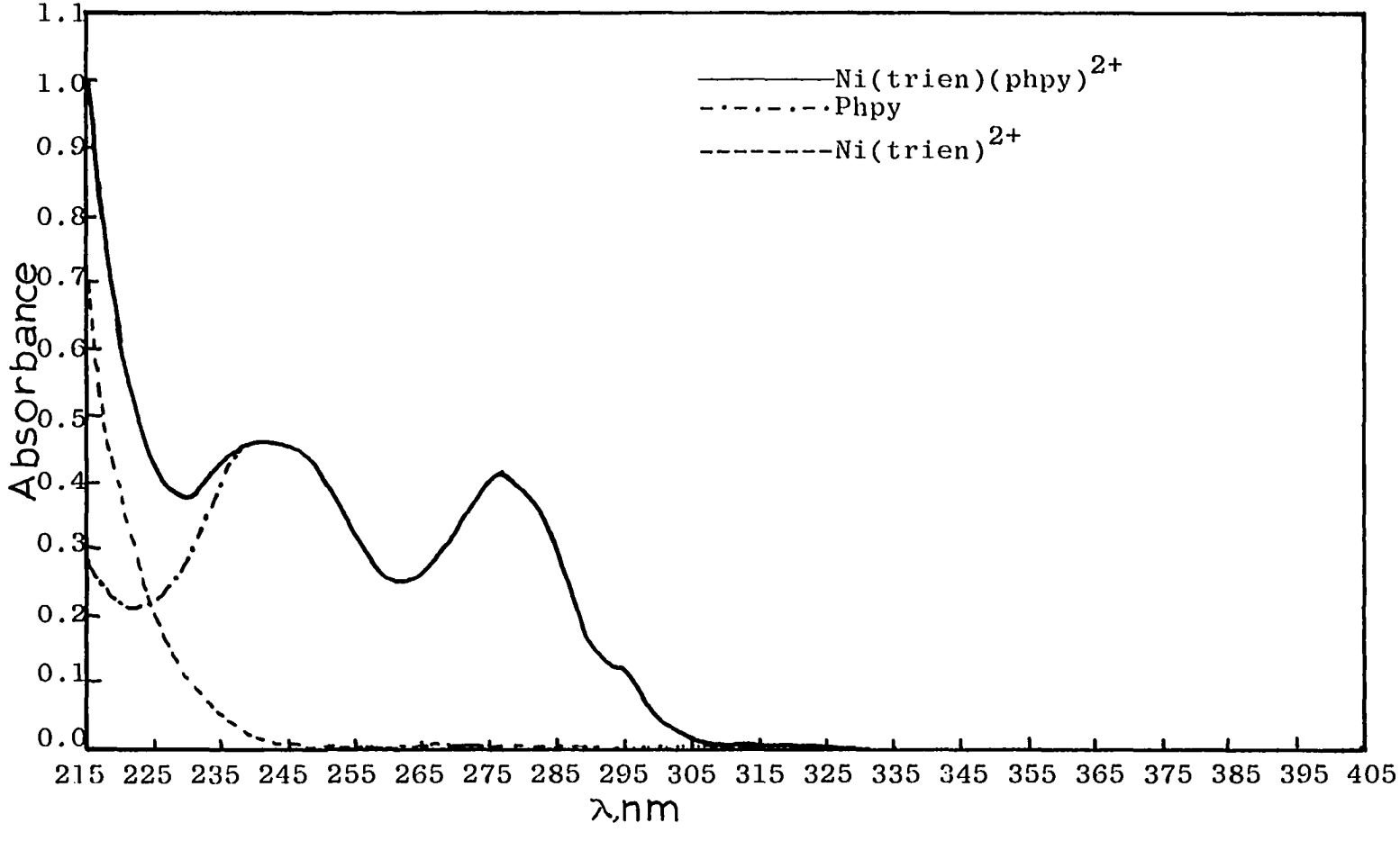

Figure 10. Absorption Spectra of $Ni(trien)^{2+}$, phpy and $Ni(trien)^{2+}$ plus phpy in 60% v/v Methanol-Water at pH = 8.7, μ = 0.1 M, C = 2.0 x 10^{-5} M, b = 2 cm

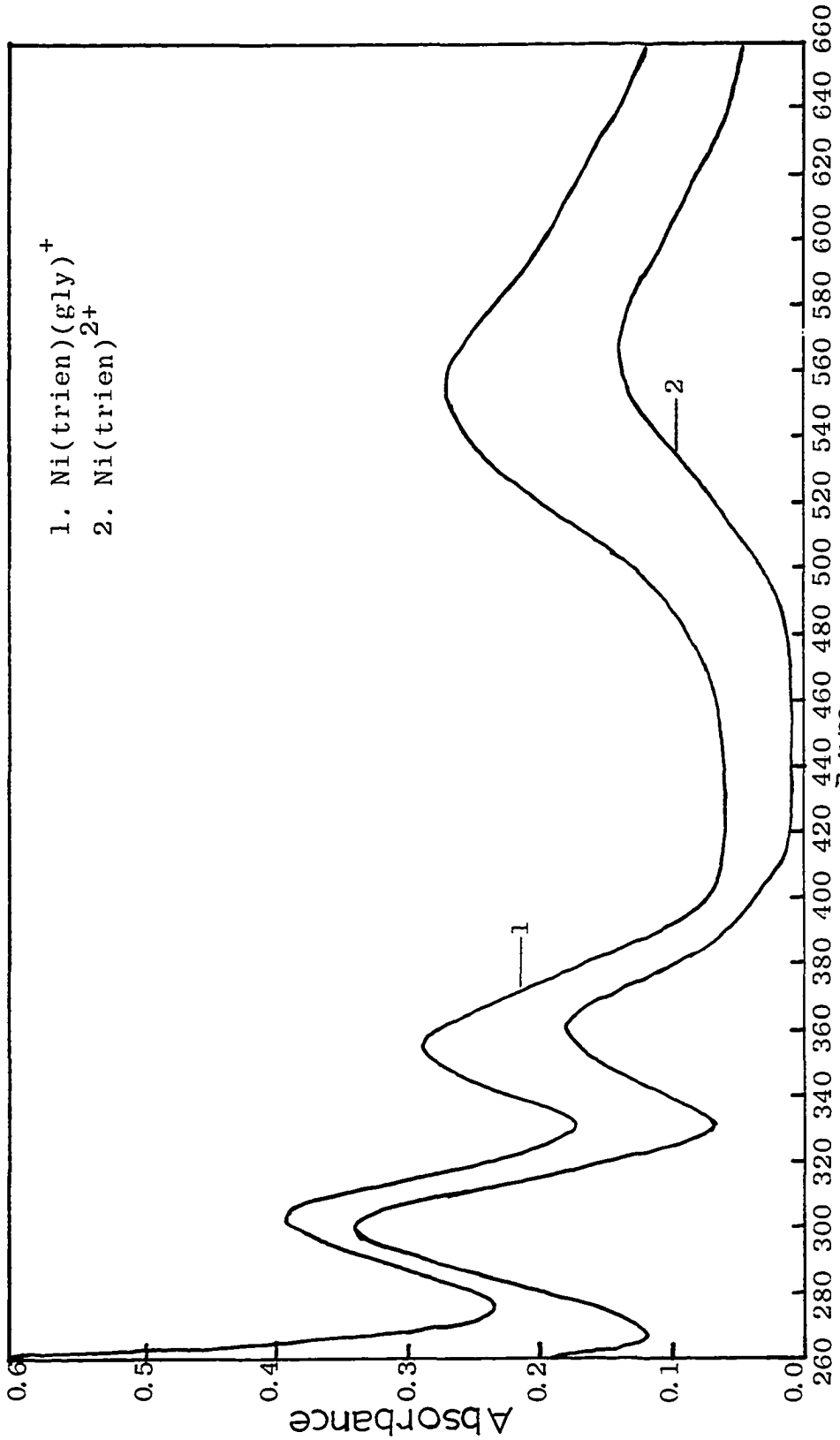

Figure 11. Absorption Spectra of $Ni(trien)^{2+}$ and $Ni(trien)(gly)^{+}$
b = 10 cm, C = 2 x 10^{-3} M, μ = 0.1 and pH 9.7

between the wavelength of 260 and 660 nm and are shown in Fig. 11. The absorption of gly in the range of the wavelengths stated was negligible. The spectra indicate, by a slight shifting of the maxima and increase of molar absorptivity of all of the absorption bands, the formation of $Ni(trien)(gly)^{+}$. The largest difference in molar absorptivity between $Ni(trien)^{2+}$ and $Ni(trien)(gly)^{+}$ is at λ = 260 nm. Therefore, this wavelength was used for kinetic runs. Table 8 gives the molar absorptivity values of the three solutions at that wavelength.

Kinetics of the reaction

Second-order runs

Stock solutions of $Ni(trien)^{2+}$ and gly were diluted to 1.2×10^{-2} M at pH 8.3. These solutions were mixed in the stopped-flow spectrophotometer and the changes in transmittance at λ = 260 nm were stored in the Biomation transient recorder and read out on a Sargent Recorder.

Pseudo first-order runs

$Ni(trien)^{2+}$ stock solution was diluted to 6.10×10^{-3} M. Glycine stock solution was diluted to 6.10×10^{-2} M, 1.22×10^{-1} M and 1.83×10^{-1} M at pH 8.2. The

TABLE 8

Spectral Data of Gly^-, $Ni(trien)^{2+}$, and $Ni(trien)(gly)^+$ at λ = 260 nm, μ = 0.1 M C = 2.0×10^{-3} M and at pH 9.7

Solution	Cell Path, cm	Abs.	ϵ	$\Delta\epsilon$
Gly^-	10	0.0	0.0	
$Ni(trien)^{2+}$	10	0.20	10	20
$Ni(trien)(gly)^+$	10	0.60	30	

kinetic runs were made and recorded as done for the second-order runs above.

Another set of solutions with a $Ni(trien)^{2+}$ concentration of 6.10×10^{-3} M and gly concentrations of 6.10×10^{-2}, 1.83×10^{-1}, and 3.05×10^{-1} M, all at pH 7, were prepared and kinetic studies were carried out.

The pH dependency of the reaction rate was studied at $\lambda = 260$ nm using a 6.10×10^{-3} M $Ni(trien)^{2+}$ and a 1.83×10^{-1} M gly with the pH ranging from 4.94 to 8.41.

Estimation of pK_a

A series of 4.72×10^{-3} M $Ni(trien)(gly)^{+}$ solutions at various pH's ranging from 4.2 to 11.8 were prepared by mixing equimolar volumes of $Ni(trien)^{2+}$ and gly with borate-mannitol buffers. The pH was adjusted to the desired value by adding HCl, mannitol or NaOH. The absorbance of each of these solutions was measured. The values and the plot, absorbance vs pH, are given in Table 9 and Fig. 12 respectively.

Glycine, $Ni(trien)^{2+}$, $Ni(trien)^{2+}$ plus ten-fold excess glycine, and $Ni(trien)^{2+}$ plus twenty-fold excess glycine solutions all at 4.72×10^{-3} M were prepared by diluting and mixing appropriate volumes of the stock solutions at pH 7.68. Glycine 3.0×10^{-1} M solutions at pH 4.8 and pH 9.4 were prepared. Absorbance values

TABLE 9

Absorbance-pH Values for $Ni(trien)(gly)^+$ Solutions and Their First Derivative[a]
λ = 358 nm, b = 10 cm, C = 4.72 x 10^{-3} M and μ = 0.1 M

pH	$\overline{pH}$	pH	A	ΔA	ΔA/ΔpH
4.20			0.093		
	4.49	0.58		0.104	0.179
4.78			0.197		
	4.89	0.22		0.101	0.459
5.00			0.298		
	5.11	0.22		0.074	0.336
5.22			0.372		
	5.36	0.28		0.024	0.086
5.50			0.396		
	5.69	0.38		0.044	0.116
5.88			0.440		
	6.05	0.34		-0.004	-0.012
6.22			0.436		
	6.37	0.30		0.018	0.060
6.52			0.454		
	6.76	0.48		0.013	0.027
7.00			0.467		
	7.21	0.41		0.028	0.068
7.41			0.495		
	7.57	0.32		0.041	0.128
7.73			0.536		
	8.02	0.57		0.047	0.082
8.30			0.583		
	8.52	0.43		0.036	0.084
8.73			0.619		
	9.03	0.60		0.027	0.045
9.33			0.646		
	9.51	0.35		0.016	0.046
9.68			0.662		
	9.91	0.45		0.040	0.089
10.13			0.702		
	10.43	0.59		0.022	0.037
10.72			0.724		
	11.27	0.10		0.019	0.018
11.82			0.743		

a. A plot A/ $\overline{pH}$ is given in Figure 20.

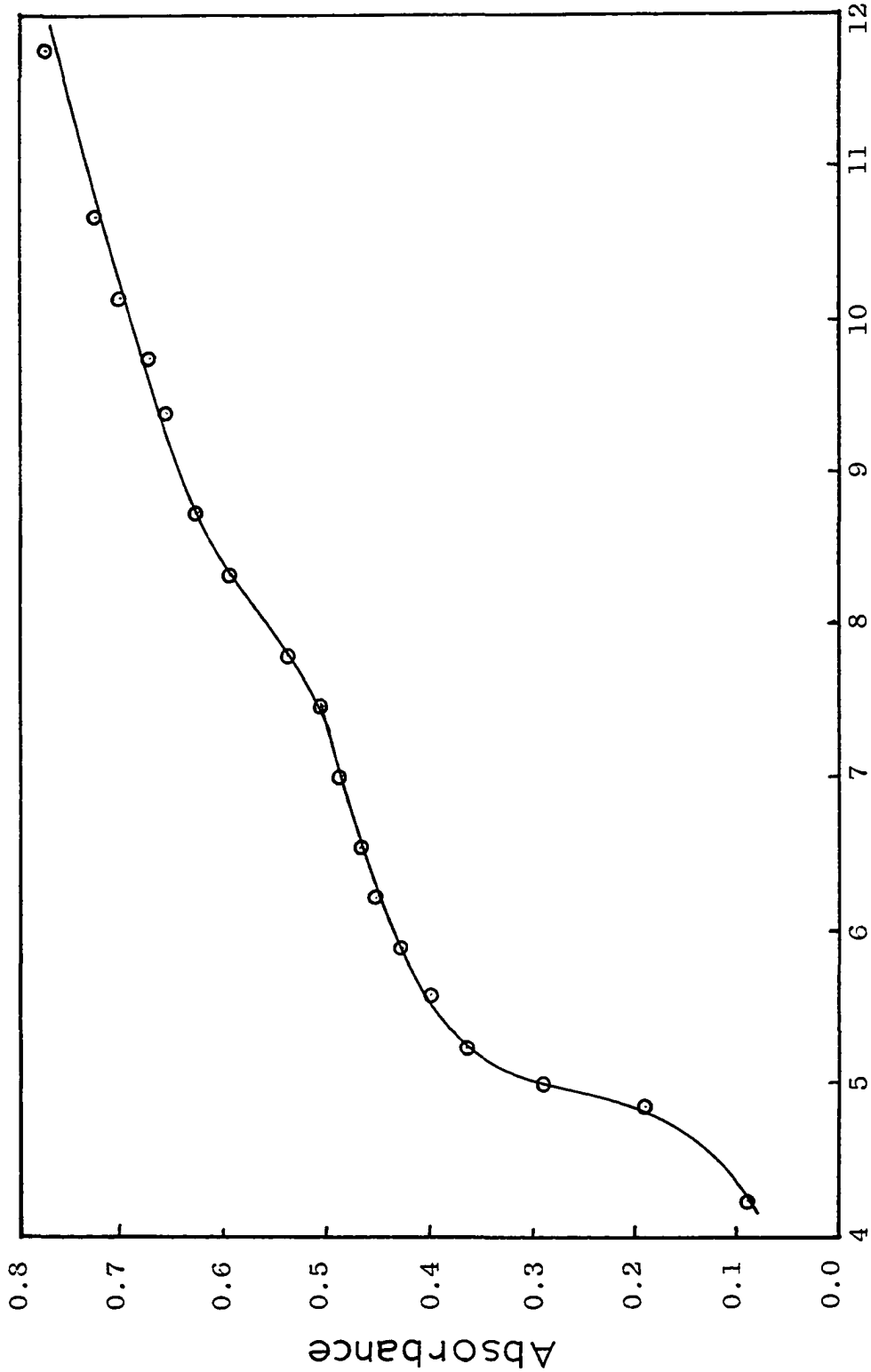

Figure 12. pH Dependency of $Ni(trien)(gly)^{+}$ Complex Shown in Absorbance. λ = 358 nm, b = 10 cm, C = 4.72 x 10^{-3} M and μ = 0.1 M

of these solutions were obtained at λ= 358 nm.

Triethylenetetramine Nickel(II) And 2-Pyridinecarboxylic Acid

Spectrophotometric study

Stock solutions of $Ni(trien)^{2+}$ and pyc were diluted to 4.0 x 10^{-5} M and pH was adjusted to 8.2 and 9.9 respectively. A solution of $Ni(trien)(pyc)^{+}$ was prepared according to eq. 9 by mixing equimolar volumes of $Ni(trien)^{2+}$ and pyc stock solutions to give a

$$Ni(trien)^{2+} + pyc^{-} \rightleftharpoons Ni(trien)(pyc)^{+} \qquad (9)$$

4.0 x 10^{-5} M solution at pH 9.8. The absorption spectra, given in Fig. 13, show the largest difference in molar absorptivity to be at a wavelength of 234 nm. Both $Ni(trien)^{2+}$ and pyc have the same molar absorptivities at this wavelength. The actual molar absorptivity values at 234 nm are listed in Table 10.

Kinetics of the reaction

Second-order runs

Two sets of different concentrations and pH's were tried. Runs at 1.51 x 10^{-4} M of $Ni(trien)^{2+}$ and pyc at pH 8.8 and μ = 0.1 M and at 2.0 x 10^{-3} M of $Ni(trien)^{2+}$ and pyc at pH 6.9 and μ = 0.1 M were mixed in the stopped-flow spectrophotometer. The transmittance changes were

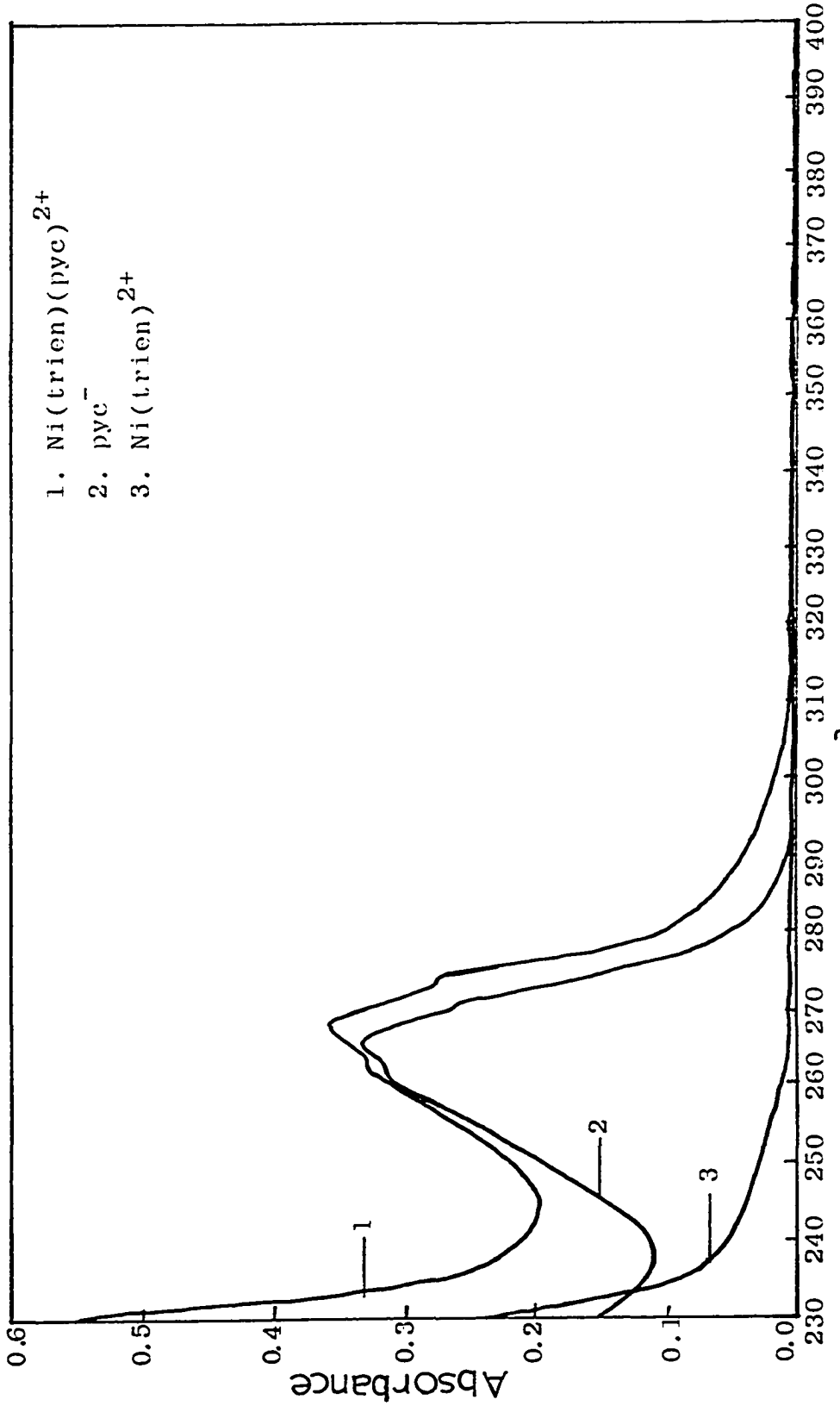

Figure 13. U. V. Absorption Spectra of Ni(trien)$^{2+}$, pyc^{-} and Ni(trien)(pyc)$^{+}$ at pH 9.8, b = 2 cm, C = 4.0×10^{-5} M

TABLE 10

Spectral Data of Pyc^-, $Ni(trien)^{2+}$, and $Ni(trien)(pyc)^+$ at λ = 234 nm, μ = 0.1 M
C = 4.0×10^{-5} M and b = 2 cm

Solution	pH	Abs.	ϵ	$\Delta\epsilon$
pyc^-	9.9	0.113	1413	
$Ni(trien)^{2+}$	8.2	0.113	1413	2500
$Ni(trien)(pyc)^+$	9.8	0.313	3913	

stored in the Biomation transient recorder and read out on a Sargent Recorder.

Pseudo first-order runs

A stock solution of $Ni(trien)^{2+}$ was diluted to 4.75×10^{-5} M. Ten-, twenty-, and thirty-fold excess pyc solutions relative to $Ni(trien)^{2+}$ were prepared by diluting appropriate volumes of pyc stock solution. The pH's of the kinetic runs of these solutions were in the range of 6-7. The pH dependency of the reaction rate was studied by carrying out kinetic runs at various pH values ranging from 4.9 to 8.8 at λ= 234 nm using a ten-fold excess of pyc^-.

CHAPTER IV

RESULTS

All the observed rate constants and mean values of replicate runs are collected in Table 11.

Triethylenetetramine Nickel(II) And 1,10-Phenanthroline

First-order rate plots were made from the integrated form of the rate equation 10, where NiT is $Ni(trien)^{2+}$

$$\frac{-d[NiT]}{dt} = k_f [NiT][phen] = k_{obsd} [NiT] \qquad (10)$$

and k_{obsd} is equal to the product of a constant and [phen]. The integrated expression of eq. 10 is

$$-\log [NiT] = \frac{1}{2.303} (k_{obsd}\, t + \text{constant}) \qquad (11)$$

Plots of -log A, proportional to -log [NiT], gave straight lines with a slope of $k_{obsd}/2.303$ from which k_{obsd} and k_f can be calculated. A typical plot is shown in Fig. 14.

Second-order rate plots were made from the integrated form of equation 12, given in eq. 13. Both reactants were present in equal concentrations.

$$\frac{-d[NiT]}{dt} = k_f [NiT][phen] \qquad (12)$$

$$\frac{1}{[NiT]} = k_f t + \text{constant} \qquad (13)$$

The relationship between [NiT] and measured absorbance

TABLE 11

Results for the Formation Reaction of $Ni(trien)^{2+}$ with Bidentate Ligands at 25° and μ = 0.1 M

$Ni(trien)^{2+}$, M	Ligand, M	pH	k_{obsd}, sec^{-1}	Mean k_{obsd}, sec-1	k_f, $M^{-1}sec^{-1}$	Mean k_f, $M^{-1}sec^{-1}$
		A. $Ni(trien)^{2+}$ with phenanthroline				
7.50×10^{-5}	7.50×10^{-4}	8.7	18.0		2.48×10^{4}	
7.50×10^{-5}	1.50×10^{-3}	8.7	47.5		3.16×10^{4}	$(2.85\pm0.24)\times10^{4}$
7.50×10^{-5}	2.25×10^{-3}	8.7	65.2		2.90×10^{4}	
1.50×10^{-3}	1.50×10^{-3}	8.8	2.36×10^{4}		2.36×10^{4}	
1.50×10^{-3}	1.50×10^{-3}	8.5	1.96×10^{4}		1.96×10^{4}	$(2.25\pm0.20)\times10^{4}$
1.50×10^{-3}	1.50×10^{-3}	8.2	2.44×10^{4}		2.44×10^{4}	
		B. $Ni(trien)^{2+}$ with bipyridyl				
5.00×10^{-5}	5.00×10^{-4}	8.8	2.99		5.98×10^{3}	
5.00×10^{-5}	1.00×10^{-3}	8.8	6.14		6.14×10^{3}	$(6.14\pm0.12)\times10^{3}$
5.00×10^{-5}	1.50×10^{-3}	8.8	9.41		6.30×10^{3}	
		C. $Ni(trien)^{2+}$ with glycine				
6.0×10^{-3}	6.0×10^{-3}	8.3	46	46[a]		

Table 11 continued

$3.1x10^{-3}$	$3.1x10^{-2}$	8.31	80	
$3.1x10^{-3}$	$6.2x10^{-2}$	8.24	89	85
$3.1x10^{-3}$	$9.3x10^{-2}$	8.22	87	
$3.1x10^{-3}$	$3.1x10^{-2}$	6.94	26	
$3.1x10^{-3}$	$9.3x10^{-2}$	6.93	21	26
$3.1x10^{-3}$	$1.6x10^{-1}$	6.92	32	
$3.1x10^{-3}$	$9.3x10^{-2}$	4.94	151	
		5.33	8.1	
		5.63	8.3	
		5.76	10.8	
		5.93	14.0	
		6.06	15.8	
		6.17	14.3	
		6.44	20	
		7.18	32	
		7.63	62	
		7.87	73	
		8.13	80	
		8.29	119	
		8.30	85	
		8.41	86	

Table 11 continued

		D. $Ni(trien)^{2+}$ with 2-pyridinecarboxylic acid		
$1.51x10^{-4}$	$1.51x10^{-4}$	8.8	50	50[a]
$2.37x10^{-5}$	$2.37x10^{-4}$	7.01	77	
$2.37x10^{-5}$	$4.75x10^{-4}$	6.97	81	82
$2.37x10^{-5}$	$7.11x10^{-4}$	6.95	88	
$2.37x10^{-5}$	$2.37x10^{-4}$	6.039	75	
$2.37x10^{-5}$	$4.75x10^{-4}$	6.066	85	80
$2.37x10^{-5}$	$7.11x10^{-4}$	6.081	80	
$2.37x10^{-5}$	$2.37x10^{-4}$	4.964	37	
		5.086	14	
		5.168	22	
		5.175	61	
		5.201	36	
		5.345	46	
		5.457	56	
		5.674	57	
		5.812	64	
		6.008	67	
		6.039	75	
		6.880	69	
		7.010	77	
		7.544	75	

Table 11 continued

	8.062 68
	8.008 79

a. Rate constant obtained by first-order plot

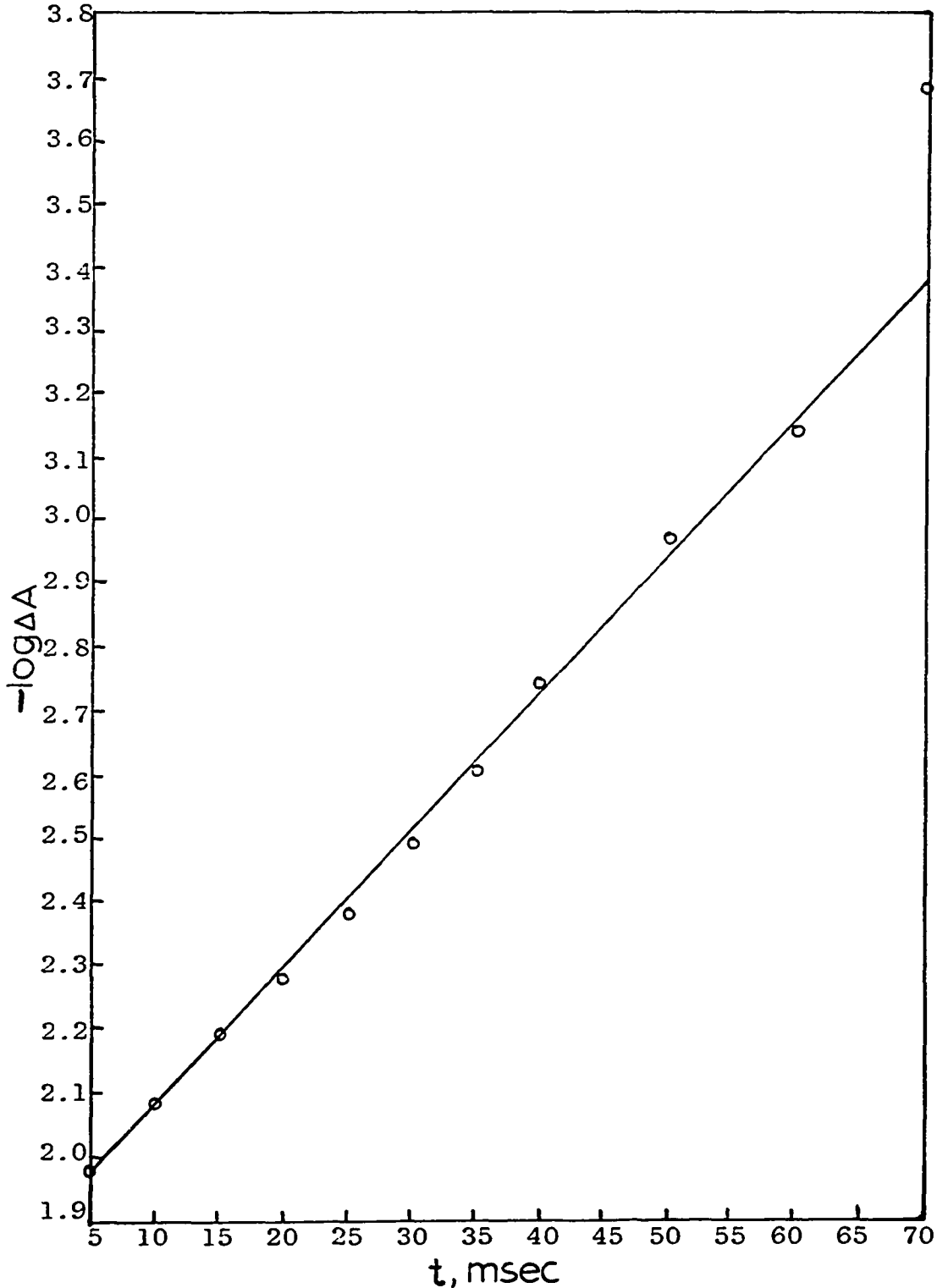

Figure 14. A Typical First-Order Rate Plot
$[NiT] = 7.50 \times 10^{-5}$ M, $[phen] = 1.50 \times 10^{-3}$ M
pH 8.7, μ = 0.1 M, Temp = 25±0.5°C

values is shown in the Appendix. Plots of 1/[Nit] vs t gave straight lines with a slope of k_f. A typical plot is shown in Fig. 15. The formation reaction between $Ni(trien)^{2+}$ and phen is thus first-order in both $Ni(trien)^{2+}$ and phen.

Triethylenetetramine Nickel(II) and 2,2'-Bipyridyl

The kinetics was found to be identical with that of $Ni(trien)^{2+}$ and phen. The data were treated according to eq. 11 or 13 depending upon which conditions applied. The reaction between $Ni(trien)^{2+}$ and bipy was shown to be first-order in both $Ni(trien)^{2+}$ and bipy.

Triethylenetetramine Nickel(II) and Ethylenediamine

The titration of the hydrochloride salt of ethylenediamine showed that the salt has a formula of en·2HCl.

Kinetic runs of the reaction between $Ni(trien)^{2+}$ and en, carried out at pH values ranging from 10 to 11, showed complicated kinetic behavior which was seen under all conditions applied. Several changes in absorbance as a function of time were detected. It was not possible to identify any one of these with the formation of $Ni(trien)(en)^{2+}$.

Triethylenetetramine Nickel(II) and n-Propylamine

Although the absorption spectra of $Ni(trien)^{2+}$ and

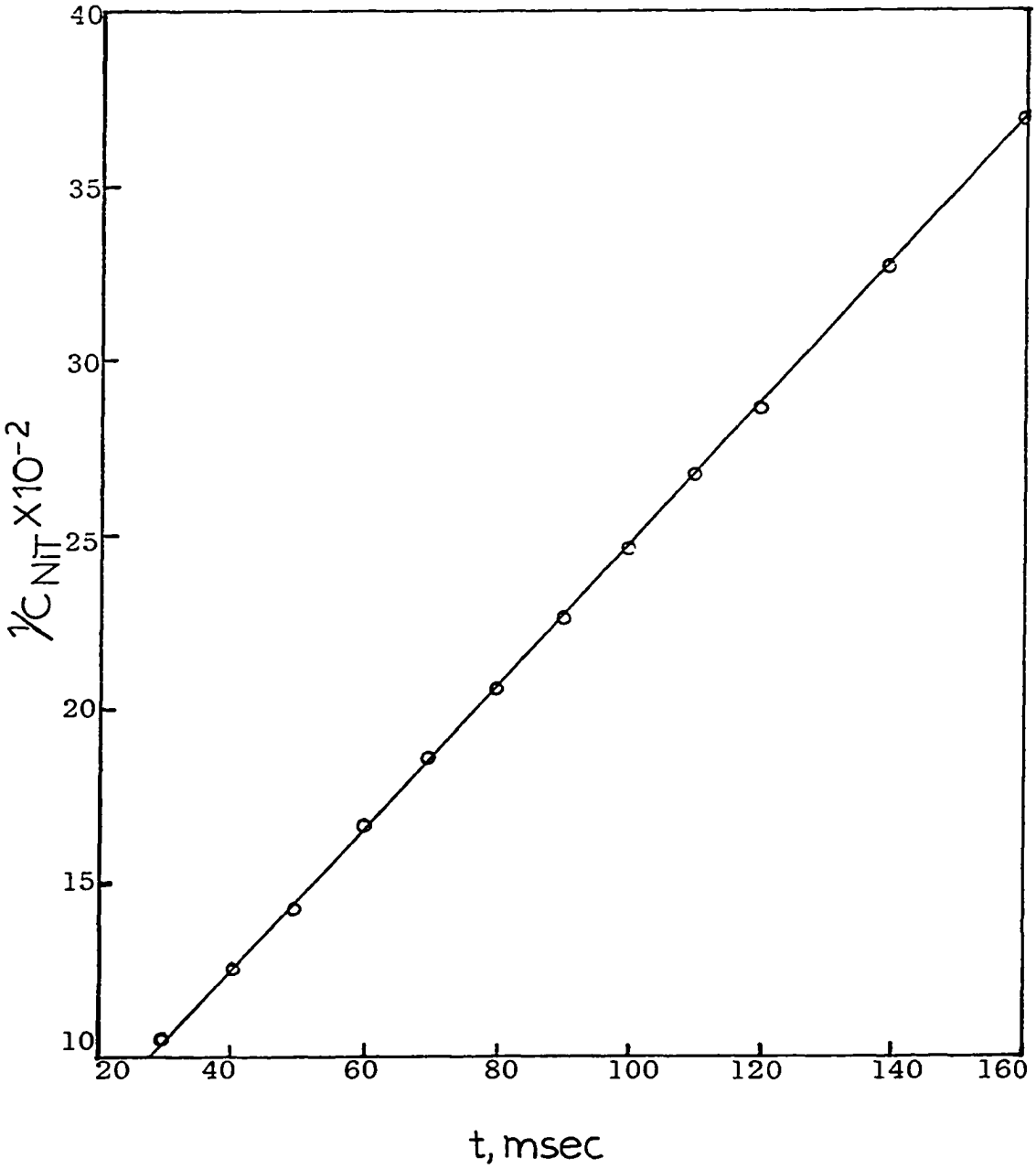

Figure 15. A typical Second-Order Rate Plot
[NiT] = 1.50 x 10^{-3} M = [phen]
pH 8.5, μ = 0.1 M, Temp = 25±0.5°C

$prNH_2$ showed the formation $Ni(trien)(prNH_2)^{2+}$, the changes in molar absorptivity were not large enough to allow measurements of the rate of formation of $Ni(trien)(prNH_2)^{2+}$.

Triethylenetetramine Nickel(II) And 7,8-Benzoquinoline

Since the spectra shown in Figs. 6 and 9 indicated that no reaction between $Ni(trien)^{2+}$ and benzoquinoline had occurred, nothing more was attempted.

The pK_a value estimated in 60% methanol-water (3.1) was somewhat higher than the value in 50% dioxane-water mixed solvent (2.7).

Triethylenetetramine Nickel(II) And 2-Phenylpyridine

Results here were identical to those for benzoquinoline. The estimated pK_a value in 60% methanol-water is 3.9 which is somewhat higher than that of benzoquinoline.

Triethylenetetramine Nickel(II) and Glycine

Absorbance with time data from kinetic runs having equal concentrations of $Ni(trien)^{2+}$ and glycine were plotted according to eq. 13. The plots (see eq. 6 of Appendix for relationship between [NiT] and measured absorbance) showed a curve with an increasing slope. The same data were then plotted according to eq. 11 assuming

gly to be zero-order. These plots gave a reasonably good straight line considering that, under the conditions, the reaction may not have gone to completion. A value of the stability constant is not available and integrated first-order rate equations for reversible systems require the equilibrium constant.

The pseudo first-order runs of ten-, twenty-, thirty-, and fifty-fold excess glycine concentration relative to $Ni(trien)^{2+}$ showed no dependence of k_{obs} on glycine concentration. Thus, the reaction is zero-order in glycine and first-order in $Ni(trien)^{2+}$ species. The only explanation for this behavior is a very rapid and therefore undetected formation of $Ni(trien)(gly)^{+}$ (or $Ni(trien)(gly)^{2+}$ depending on pH) with only one of the two dentate sites of glycine bonded to $Ni(trien)^{2+}$. The observed absorbance changes are then due to ring closure involving the second dentate site of glycine bonding to the nickel complex.

Resolution of the rate constants for the formation reaction

The pH dependency of k_{obsd} is shown in Table 11. A plot of k_{obsd} vs pH, shown in Fig. 16, resembles an acid-base titration curve with the point of inflection near pH 7.6. The pH dependency of k_{obsd} can be explained as resulting from a protonated and unprotonated form of

$Ni(trien)(gly)^{2+}$ undergoing a rate-determining ring closing step as shown in eq. 14 (omitting charges for the sake of convenience) where $[NiTG]_T$ represents total

$$k_{obsd}[NiTG]_T = k_1[NiTGH] + k_2[NiTG] \quad (14)$$

Ni(trien)(gly) species in solution. Substituting from eqs. 15 and 16,

$$K_a = \frac{[NiTG][H^+]}{[NiTGH]} \quad (15)$$

$$[NiTG]_T = [NiTG] + [NiTGH] \quad (16)$$

both equations 17 and 18 result, which allows resolution of k_1 and k_2, where k_1 is the rate constant for protonated glycine and k_2 is that for unprotonated glycine.

$$k_{obsd}(1 + \frac{[H^+]}{K_a}) = k_1(\frac{[H^+]}{K_a}) + k_2 \quad (17)$$

$$k_{obsd}(1 + \frac{K_a}{[H^+]}) = k_1 + k_2(\frac{K_a}{[H^+]}) \quad (18)$$

A plot of $k_{obsd}(1 + \frac{[H^+]}{K_a})$ vs $[H^+]$ shown in Fig. 17, gives a straight line with a slope of k_1/K_a. The value of K_a was estimated experimentally and described in the next section. The y-intercept represents the formation rate constant (k_2) for the unprotonated species of NiTG. However, since there is less uncertainty in the slope than in the y-intercept, k_2 can also be obtained from the slope of the plot of equation 18 as shown in Fig. 18. A least-square-fit was used to plot and obtain the slope and the y-intercept of Figs. 17 and 18.

The values of k_1 and k_2 are listed in Table 12.

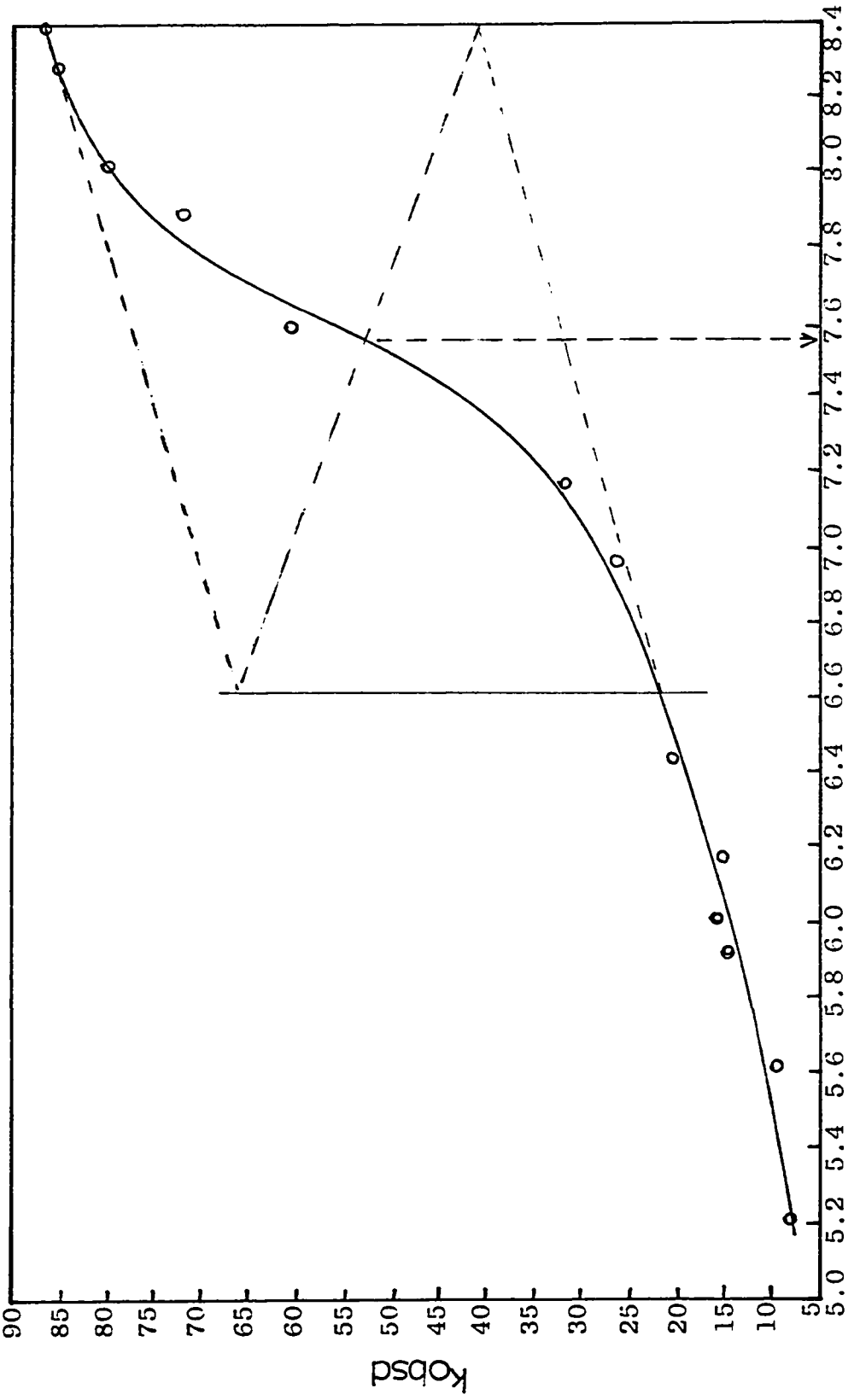

Figure 16. Dependency of k_{obsd} on pH for $Ni(trien)(gly)^+$ Formation Reaction, μ = 0.1 M, Temp = 25±0.5°C

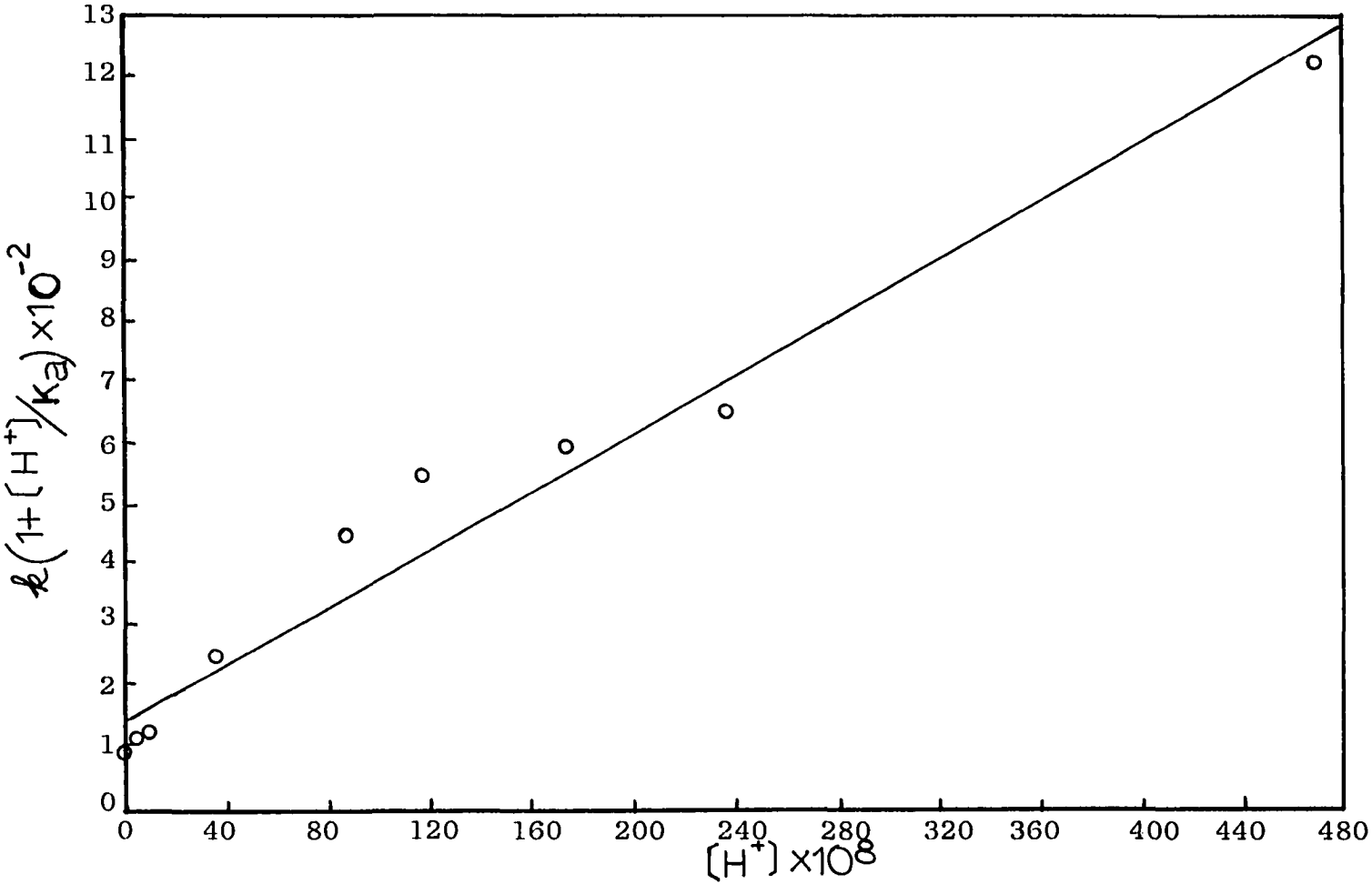

Figure 17. Resolution of Formation Rate Constants Showing pH Dependency of Reaction Rate for $Ni(trien)(gly)^+$ Formation Reaction
μ = 0.1 M, Temp =25±0.5°C

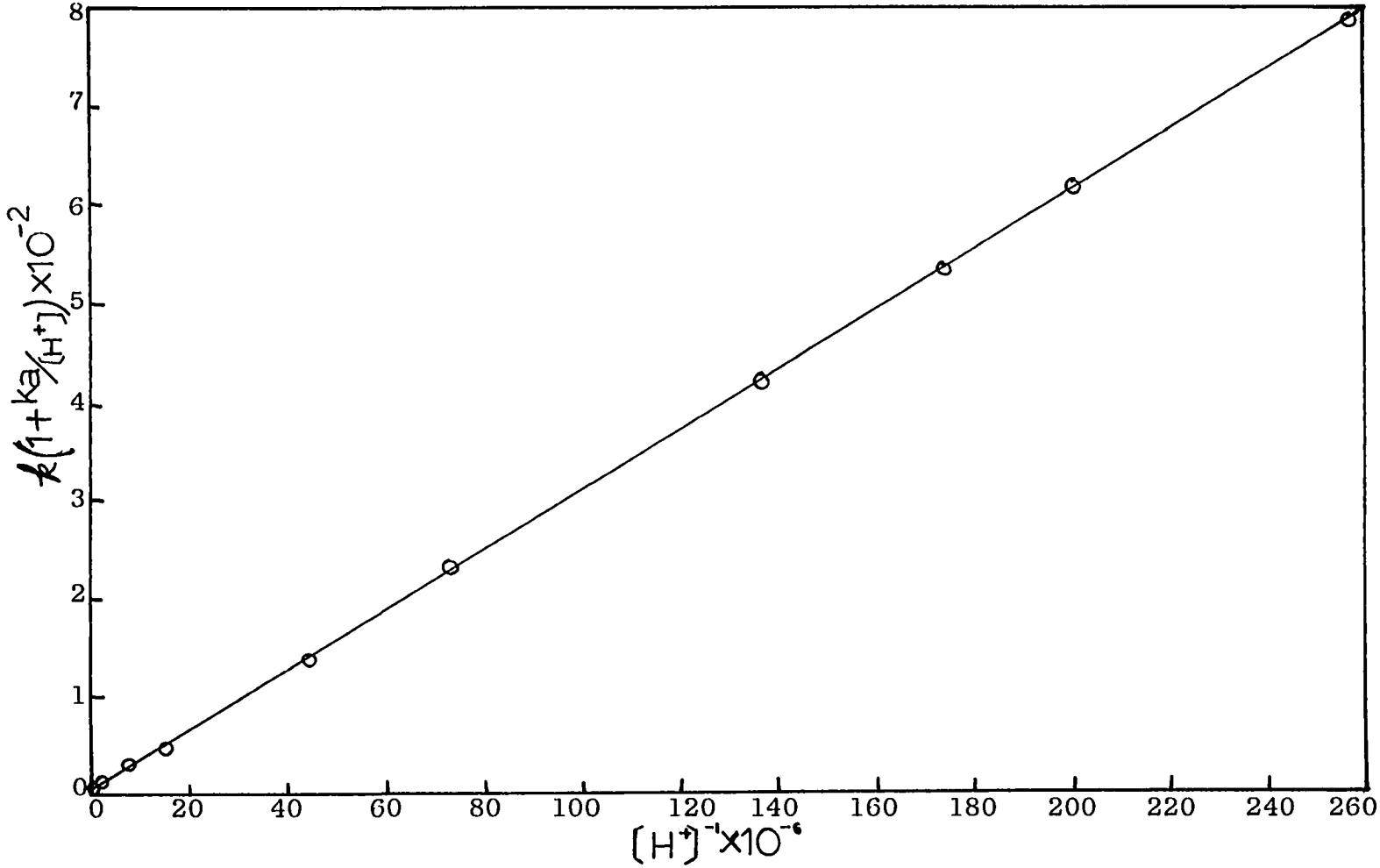

Figure 18. Resolution of Formation Rate Constants Showing pH Dependency of the Reaction Rate for $Ni(trien)(gly)^+$ Formation Reaction, μ = 0.1 M, Temp = $25\pm0.5^{o}C$

TABLE 12

Resolved Rate Constants[a] of the Formation Reactions of Glycine and 2-Pyridinecarboxylic Acid with $Ni(trien)^{2+}$ At 25° and μ = 0.1 M

Ligand	Ka, M	k_1, sec^{-1}	k_2, sec^{-1}
gly	3.16×10^{-8}	7.6 ± 0.4	96 ± 0.5
pyc	3.2×10^{-6}	23 ± 2.3	78 ± 0.4

a. The uncertainties correspond to standard deviations for least-square-fit.

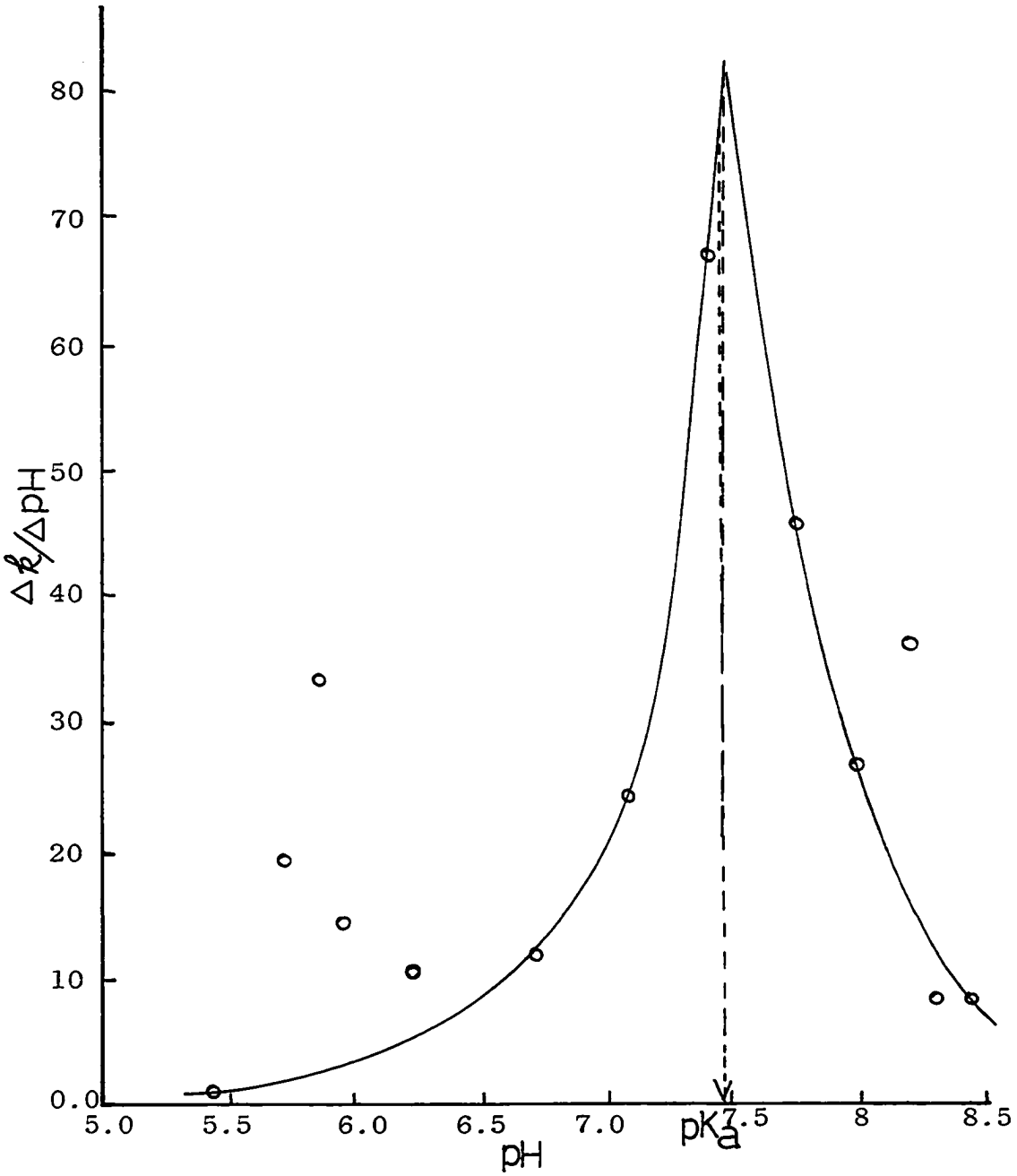

Figure 19. Estimation of pK_a Value for $Ni(trien)(gly)^+$ Formation Reaction from the Rate Data

Estimation of K_a value

The inflection point of the plot of k_{obsd} vs pH (Fig. 16) lies around pH 7.6 which corresponds to a pK_a value of Ni(trien)(gly H)$^{2+}$. The first derivative plot of Fig. 16 was made to locate more precisely the point of inflection and this is shown in Fig. 19. The inflection point obtained from Fig. 19 occurs at pH = 7.45 and is in close agreement with the estimated pK_a value obtained from Fig. 16.

The absorbance of solutions containing a 1:1 ratio of Ni(trien)$^{2+}$ and glycine was measured as a function of pH. A plot of these data (Table 9) shown in Fig. 12 gives an inflection point at a pH of around 7.6-8. The first derivative of this plot, shown in Fig. 20, gives a pK_a value of 7.55. It is interesting to note that this value is close to the pK_a (7.45) found for Ni(trien)(gly H)$^{2+}$. The mean value of 7.55 and 7.45 is 7.5 and is assigned as pK_a for formation reaction of Ni(trien)$^{2+}$ and glycine. Absorbances of solutions having various ratios of Ni(trien)$^{2+}$ to glycine at a fixed pH of 7.68 were measured at λ = 358 nm. Table 13 shows the data. Ratios of Ni(trien)$^{2+}$ to glycine of 1:10 or greater show no increase in absorbance, indicating that the reaction has gone to completion.

The absorbance of a 1:1 ratio of $Ni(trien)^{2+}$ to gly, however, is less than those of the 1:10 or 1:20 ratio solutions. This indicates that the second-order kinetic runs, plotted as first-order kinetics, did not go to completion. The absorbance-pH runs from a 1:1 ratio of $Ni(trien)^{2+}$ to glycine had some reactants present which could undergo a protonation-deprotonation reaction. This would explain the dependence of absorbance upon pH.

Two solutions of glycine at pH 4.8 and 9.4 and both at a concentration of 0.30 M gave no absorption at the wavelength 358 nm.

Triethylenetetramine Nickel(II) And 2-Pyridinecarboxylic Acid

Plots of second-order runs (see eq. 7 of Appendix for relationship of $[Ni(trien)^{2+}]$ to absorbance) having equal concentrations of $Ni(trien)^{2+}$ and pyc^- gave curves just as in the $Ni(trien)^{2+}$—glycine system. First-order plots of the second-order runs were relatively linear, again just as the $Ni(trien)^{2+}$—glycine system.

Pseudo first-order runs were made at two different pH values with pyc concentrations of ten-, twenty-, and thirty-fold excess relative to $Ni(trien)^{2+}$. The observed rate constant failed to show any orderly dependence upon pyc^- concentration. Thus the kinetics of the reaction

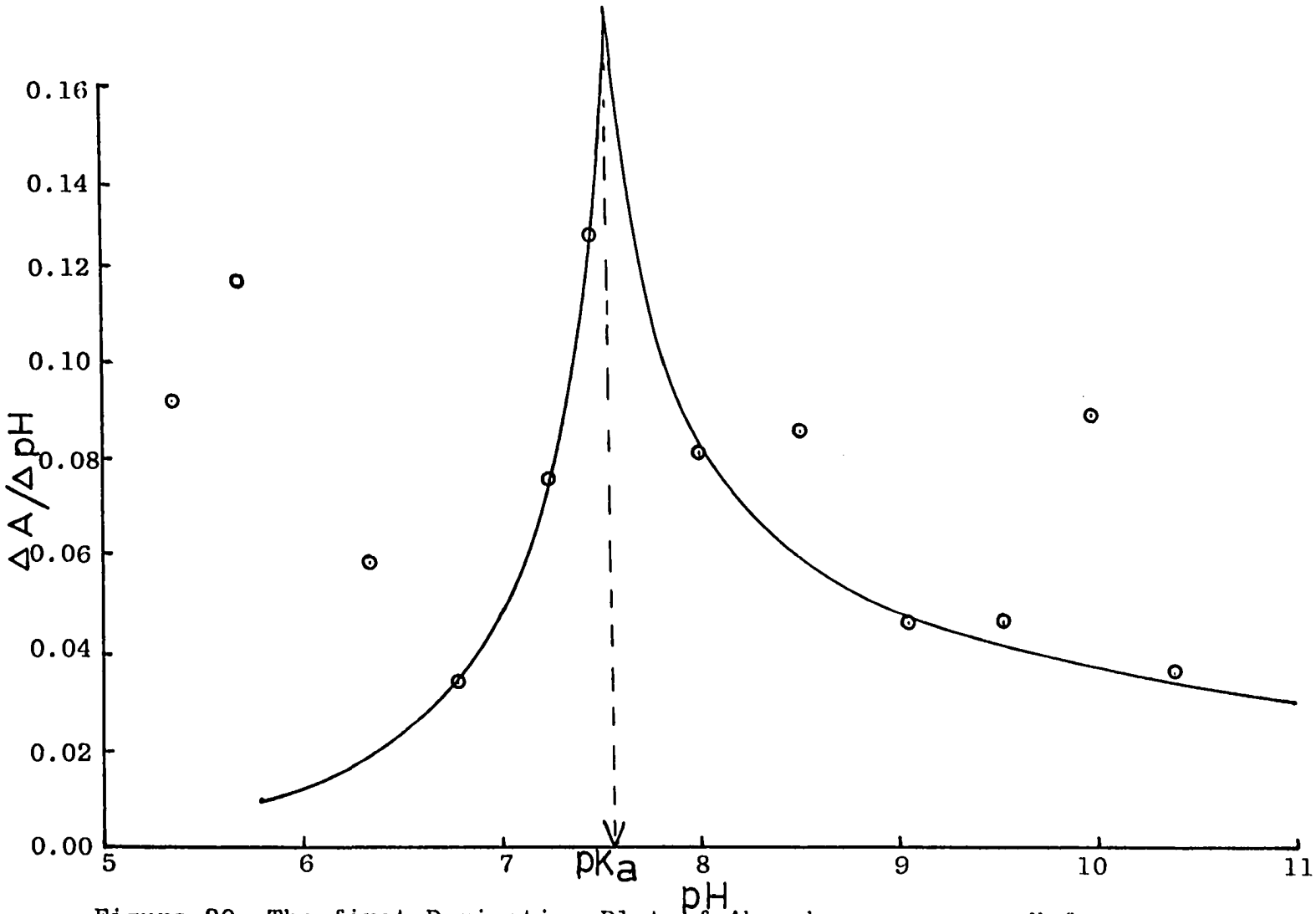

Figure 20. The first Derivative Plot of Absorbance versus pH for $Ni(trien)(gly)^{+}$ Formation Reaction

TABLE 13

Absorbance Values of Reactants and Product at λ = 358 nm With Different $Ni(trien)^{2+}$ and Glycine Ratios for the Formation Reaction

μ = 0.1 M, b = 10 cm, $[Ni(trien)^{2+}] = 4.72 \times 10^{-3}$ M, pH 7.68

Solution	$Ni(trien)^{2+}$: gly	Abs
gly^- ($C = 4.72 \times 10^{-3}$ M)		0.0
$Ni(trien)^{2+}$		0.454
$Ni(trien(gly)^+$	1 : 1	0.527
	1 : 10	0.640
	1 : 20	0.635

are identical to those of the $Ni(trien)^{2+}$--glycine system, that is, first-order in $Ni(trien)^{2+}$ species and zero-order in pyc^-.

Resolution of rate constants for the formation reaction

To determine the K_a value for the formation reaction, a plot of k_{obsd} vs pH was made and is shown in Fig. 21. The first derivative plot of Fig. 21 is shown in Fig. 22 and was used to locate a more precise pK_a value. The pK_a value estimated from Fig. 21 (5.55) and from Fig. 22 (5.45) are in close agreement and a pK_a value of 5.5 ($K_a = 3.2 \times 10^{-6}$) was assigned to the species $Ni(trien)\ (pycH)^{2+}$.

The pH dependency of k_{obsd}, shown in Fig. 21 can be explained using eq. 14 substituting pyc^- for gly^-. Plots of equations 17 and 18 using the $Ni(trien)^{2+}$—pyc data are shown in Figs. 23 and 24. Least-square-fit of the data gave the rate constants k_1 and k_2 which are listed in Table 12.

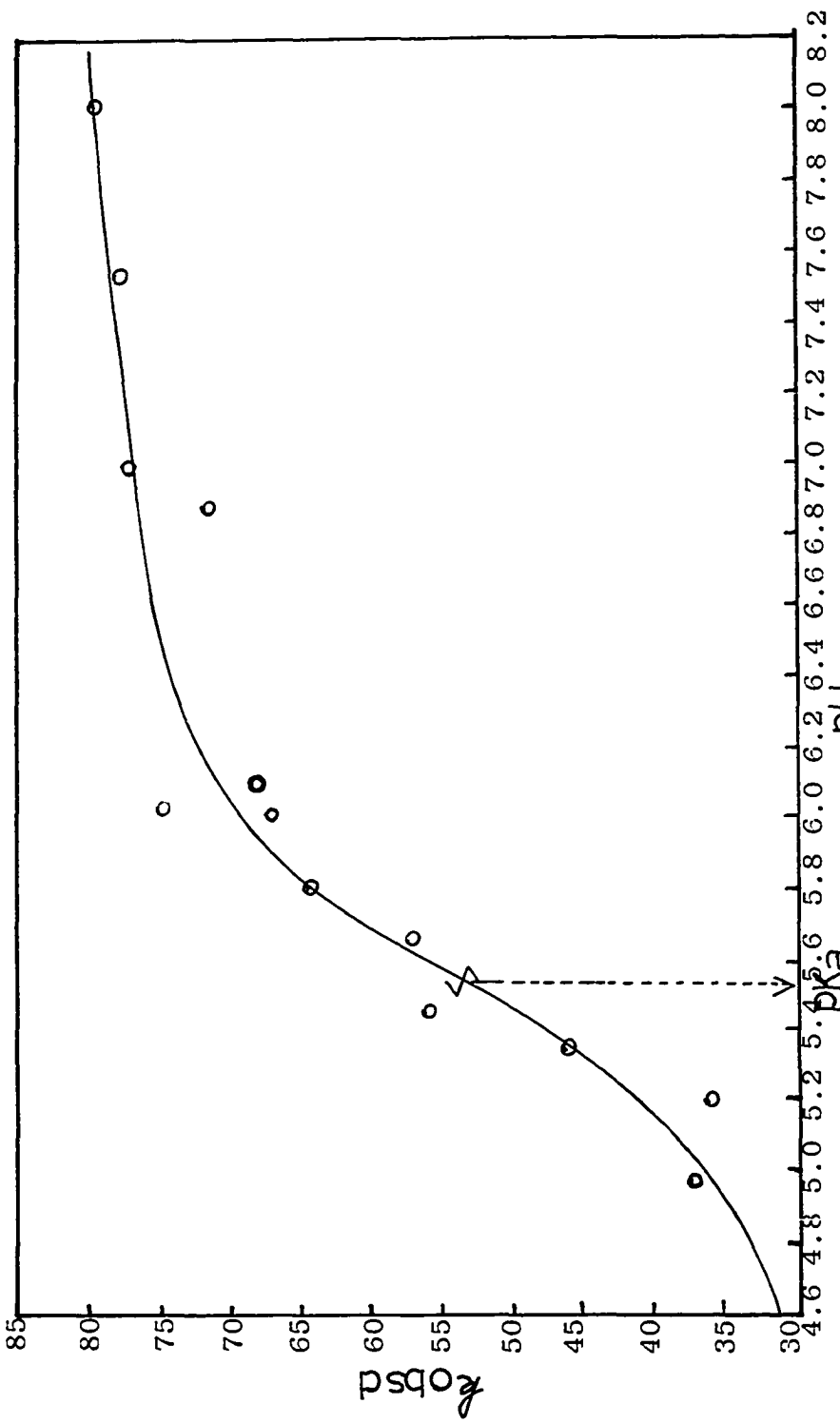

Figure 21. pH Dependency of the Observed Rate Constant for $Ni(trien)(pyc)^+$.
μ = 0.1 M, Temp = 25±0.5°C

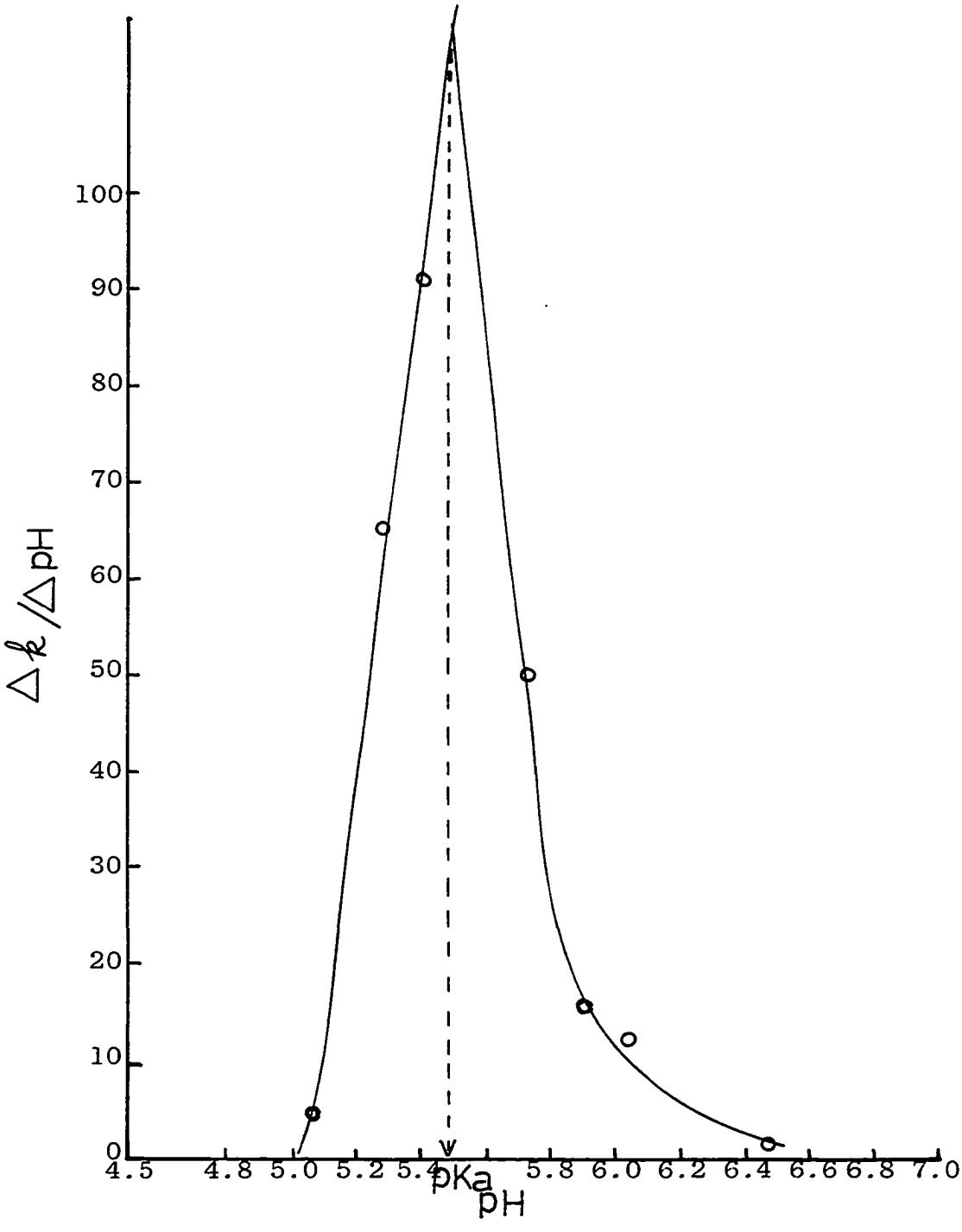

Figure 22. Estimation pK_a value for $Ni(trien)(pyc)^+$ Formation Reaction from the Rate Data

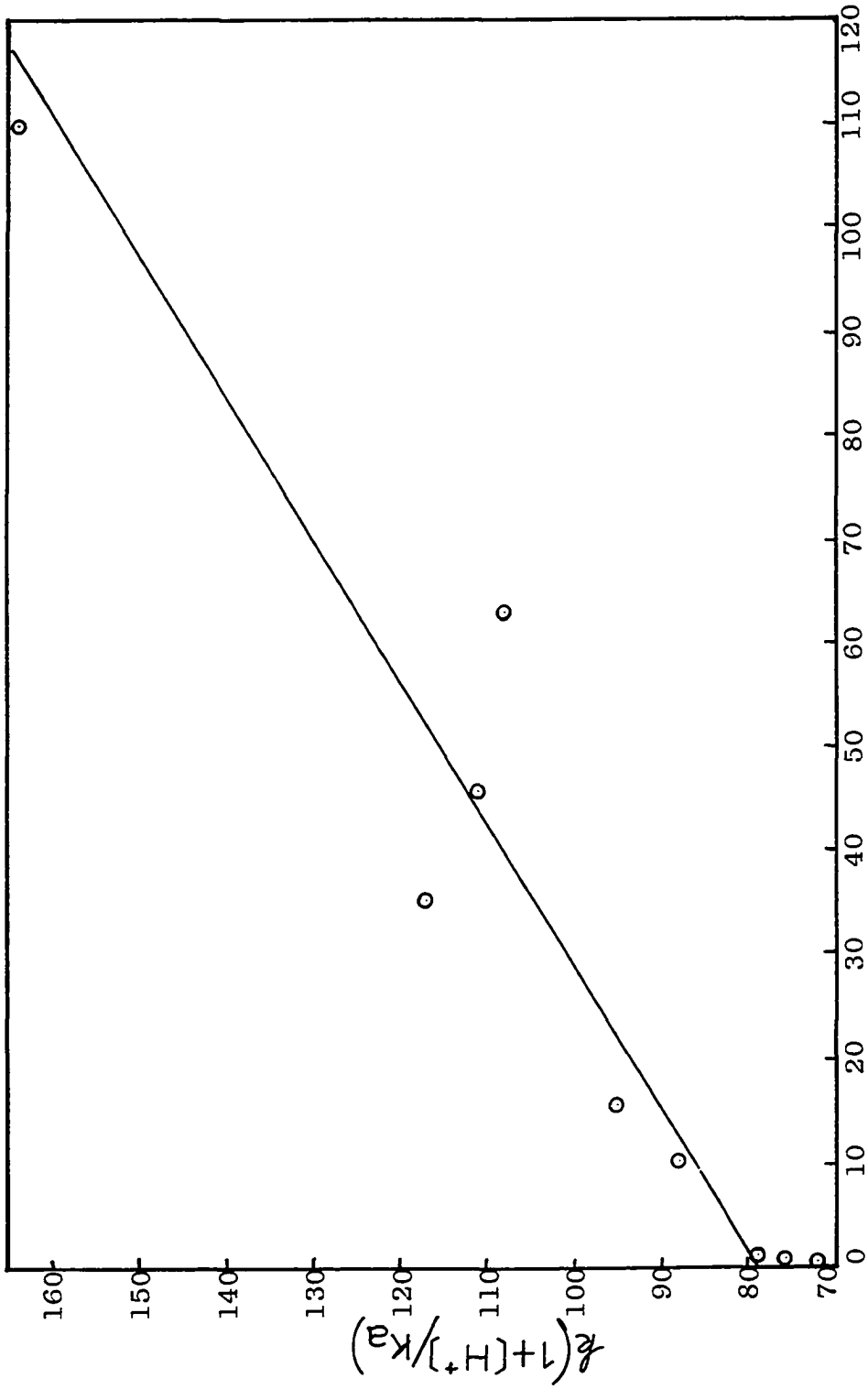

Figure 23. Resolution of Formation Rate Constants for the Reaction of $Ni(trien)^{2+}$ and 2-Pyridinecarboxylic Acid. μ = 0.1 M, Temp = 25±0.5°C

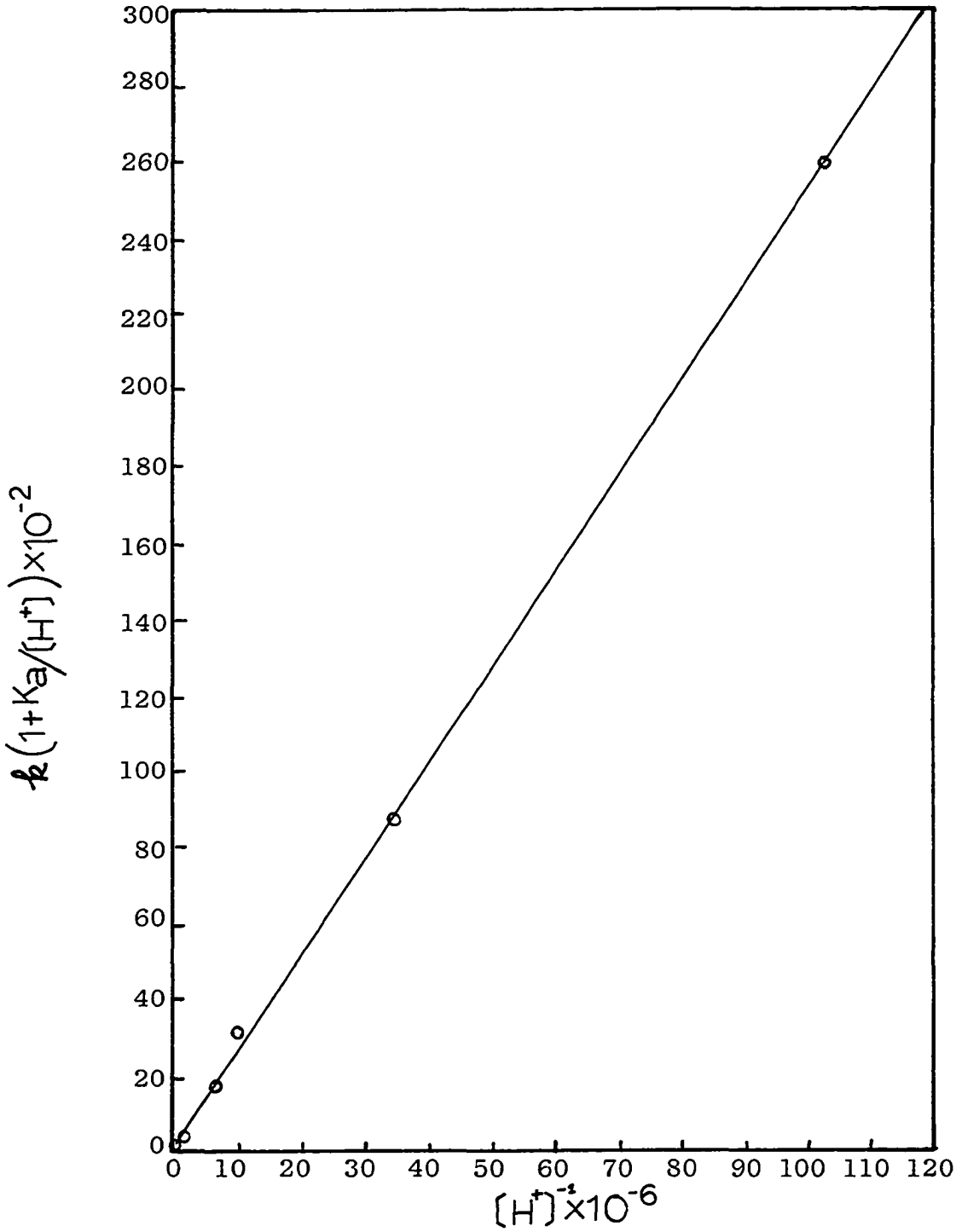

Figure 24. Resolution of Formation Rate Constants for the Reaction of $Ni(trien)^{2+}$ with 2-Pyridine-carboxylic Acid. μ = 0.1 M, Temp = 25±0.5°C

CHAPTER V

DISCUSSION

The second-order formation rate constant (k_f) is a composite value as shown in eq. 2, the product of an outer-sphere association constant (K_{os}) and a first-order rate constant (k^{-H_2O}) for water exchange of the outer-sphere complex. The assumption is made that if a chelate ring is formed, ring closure is rapid compared to loss of the initial water molecule released from the metal ion.[29-31] This assumption, however, is valid only for the case of a normal substitution process for reasons to be discussed later.

The formation reactions of $Ni(trien)^{2+}$ with a bidentate ligand are thought to occur through a series of elementary steps[6] as shown in the following equations.

$$(H_2O)Ni(trien) + L\text{-}L \underset{}{\overset{K_{os}}{\rightleftharpoons}} (H_2O)Ni(trien)(H_2O)(L\text{-}L) \quad (19a)$$

$$(H_2O)Ni(trien)(H_2O)(L\text{-}L) \underset{k_{21}}{\overset{k_{12}}{\rightleftharpoons}} (H_2O)(trien)Ni\text{-}L\text{-}L + H_2O \quad (19b)$$

$$(H_2O)(trien)Ni\text{-}L\text{-}L \underset{k_{32}}{\overset{k_{23}}{\rightleftharpoons}} (trien)Ni\overset{L}{\underset{L}{<}} + H_2O \quad (19c)$$

$k_1^{-H_2O}$ $k_2^{-H_2O}$

The charge on Ni(II) is omitted from the sake of convenience and L-L represents a bidentate ligand. Equations

19b and 19c are dissociative. The water molecules leave the inner sphere before L-L forms a bond with the central metal ion.[6,36] These observations are accounted for by a mechanism in which the ligand and the diaquated nickel ion are in rapid equilibrium with an outer-sphere complex in which the incoming ligand occupies a position in the second coordination sphere. The RDS is the collapse of this outer-sphere complex to give the inner-sphere complex. The rate law predicted by this mechanism is

$$\frac{d[(trien)Ni\overset{L}{\underset{L}{}}]}{dt} = k_f[Ni(trien)][L\text{-}L] - k_d[(trien)Ni\overset{L}{\underset{L}{}}] \quad (20)$$

where $$k_f = \frac{K_{os}k_{12}k_{23}}{k_{21} + k_{23}} \quad (20a)$$

$$k_d = \frac{k_{21}k_{32}}{k_{21} + k_{23}} \quad (20b)$$

If ring closure, step k_{23}, is rapid compared to the rupture of the Ni-L bond, k_{21} ($k_{23}/k_{21} > 1$) and assuming the position of equilibrium lies far to the right, then the experimentally observed rate law follows.

$$\frac{d[(trien)Ni\overset{L}{\underset{L}{}}]}{dt} = K_{os}k^{-H_2O}[Ni(trien)][L\text{-}L] \quad (21)$$

where $k_{12} = k^{-H_2O}$. Thus $k_f = K_{os}k^{-H_2O}$. Equation 21 is equivalent to eq. 12 for the case of phen reacting with $Ni(trien)^{2+}$. The k^{-H_2O} term then represents the

unimolecular dissociation of a water molecule from the inner coordination shell of the metal ion-ligand bond upon interaction with solvent molecules.

A reasonable approximation to K_{os} can be calculated by using the Fuoss-Eigen equation[7,8] which is expressed in eq. 22

$$K_{os} = 4/3\,\pi a^3 N_A \times 10^{-3}\, exp\frac{-U(a)}{kT} \qquad (22)$$

where U(a) is the Debye-Hückel interionic potential

$$U(a) = \frac{-Z_1 Z_2 e_o^2}{a'D} - \frac{Z_1 Z_2 e_o^2 \mathcal{K}}{DkT(1+ a')} \qquad (23)$$

and $\mathcal{K} = \frac{8\, N_A e_o^2 \mu\, \frac{1}{2}}{1000DkT}$

In the above equations, μ is the ionic strength, N_A is Avogadro's number, a is the center-to-center distance between the metal and the ligand dentate site undergoing coordination, a' is the center-to-center distance between the metal and the protonated nitrogen donor atom of the ligand, Z is the formal charge on the reacting species, e_o is the electron charge, kT is the Boltzmann energy factor, and D is the dielectric constant of the solvent.

Molecular models of $Ni(trien)^{2+}$ and the ligands used in this study show that the center-to-center distance of closest approach between the nitrogen or oxygen donor atom and $Ni(trien)(H_2O)_2^{2+}$ remains about the same as for

ammonia. Consequently, K_{os} varies only with the charge on the ligands and the formation rate constants can be predicted from eq. 2. For $Ni(trien)^{2+}$ reacting with the neutral ligands used in this study, k_f should be about the same as the value obtained with ammonia if nothing else in the mechanism affects the rate.

If a ligand is already coordinated to nickel(II), the product $K_{os}k^{-H_2O}$ must be corrected by a statistical factor.[9,29] This statistical correction accounts for the fact that less than six coordination sites are available in the complexed nickel.

$$k_f = K_{os}k^{-H_2O}\frac{(6-n)}{6} \qquad (24)$$

Here n represents the number of sites occupied by non-labile coordinated ligands on the nickel(II) and is 4 for trien.

Coordinated polyamines increase the rate of replacement of the remaining water molecules. This has been well demonstrated by Margerum and co-workers.[9,10] Triethylenetetramine coordinated to Ni(II) increases the rate of water loss by a factor of 178 (see Table 14) compared to hexaaquo nickel.

Using the estimated value of $a = 4 \times 10^{-8}$ cm, K_{os} is calculated to be 0.16 M^{-1} for uncharged ligands. The value of k^{-H_2O} for trien coordinated to Ni(II) was experimentally determined by Margerum and co-workers[10] at

TABLE 14

The Experimental and Calculated[a] Formation Rate Constants, Calculated Steric Factors[b] and Water Exchange Rate Constants of Substitution Reaction of Various Ligands with Various Nickel Complexes

Substituting Ligand	k_f exptl x 10^{-4} $M^{-1}sec^{-1}$	k_f Calcd x 10^{-4} $M^{-1}sec^{-1}$	Es	Ref.
With $Ni(H_2O)_6^{2+}$, $k^{-H_2O} = 2.8 \times 10^4$ sec^{-1}[c]				
phen	0.39	0.45	-0.06	34
Bipy	0.161	0.45	-0.15[d]	11
En	36	0.45	1.9	45
NH_3	0.43	0.45	-0.02	46
Gly^-	2.2	5.4	-0.39	47
Pyc^-	2.6	5.4	-0.32	47
With $Ni(en)^{2+}$, $k^{-H_2O} = 4.4 \times 10^4 sec^{-1}$[e]				
phen	0.95	0.70	0.13	11
Bipy	0.50	0.70	0.16[d]	11
NH_3	1.2	0.70	0.23	9, 10

TABLE 14 (Continued)

With $Ni(dien)^{2+}$, $k^{-H_2O} = 1.2 \times 10^6 sec^{-1}$[f]				
phen	2.3	19	-0.92	11
Bipy	1.1	19	-0.94[d]	11
NH_3	4.3	19	-0.65	9, 10
With $Ni(en)_2^{2+}$, $k^{-H_2O} = 5.4 \times 10^6 sec^{-1}$[e]				
phen	9.3	27	-1.46	11
Bipy	8.4	27	-0.21[d]	11
En	100[g]	27	0.57	13
With $Ni(trien)^{2+}$, $k^{-H_2O} = 5 \times 10^6 sec^{-1}$[h]				
phen	2.25	27	-1.1	This study
Bipy	0.614	27	-1.3[d]	This study
En	--[i]	27		
$PrNH_2$	--[i]	27		
$NH_3(8^o)$	12	27	-9.35	10
Gly^-	--[i]		-1.32,-1.12[j]	This study
Pyc^-	--[i]		-1.41,-0.64[j]	This study
With $Ni(tren)^{2+}$, $k^{-H_2O} = 6.9 \times 10^5 sec^{-1}$, $1.0 \times 10^7 sec^{-1}$[k]				
phen	1.3	9.6[l]	-0.87	6

TABLE 14 (Continued)

Bipy	1.0	9.6[1]	-0.68	6
NH_3(6°C)	26	9.6[1]	0.43	10
Gly^-	9.0	115[1]	-1.1	6

---

a. Calculated using eqs. 2 and 22

b. Calculated using eqs. 2 and 26

c. Ref. 10

d. Corrected for contribution due to ring closure

e. H. W. Dodgen, A. G. Desai and J. P. Hunt, J. Am. Chem. Soc., 91 5001(1969)

f. Ref. 4

g. Ref. 11, the value estimated in the study

h. Ref. 10, corrected to 25°C

i. Could not be measured in this study

j. Calculated for ring closure step of unprotonated and protonated ligand in order written in the Table using k_{ref}, unprotonated = $2x10^3 sec^{-1}$ and k_{ref}, protonated = 10^2 sec^{-1}

k. D. P. Rablen, H. W. Dodgen and J. P. Hunt, J. Am. Chem. Soc., 94, 1771(1972), the two water molecules of $Ni(tren)^{2+}$ exchange at different rates

l. Smaller k^{-H_2O} used

$8^{o}C$ but it was corrected[32] to 5×10^{6} sec^{-1} at $25^{o}C$ using $\Delta H^{\ddagger} = 7$ kcal/mol. Then k_f, calculated from eq. 24, becomes $2.7 \times 10^{5} M^{-1} sec^{-1}$ for all uncharged ligands used in this study.

Coordination of ethylenediamine or diethylenetriamine[11] to Ni(II) substantially increased the rates of formation of aromatic ligands relative to $Ni(H_2O)_6^{2+}$. The rate constants for these reactions and their water-exchange rates are listed in Table 14. Although the rate of water loss of the polyamine nickel(II) complexes increased regularly, these increases are not shown as dramatically in the formation rates of phenanthroline and bipyridyl. Formation rate constants actually decreased from $Ni(dien)^{2+}$ to $Ni(en)_2^{2+}$. This indicates the importance of the coordinated ligand in affecting the formation rate constant.

Triethylenetetramine Nickel(II) With Phenanthroline and Bipyridyl

The experimental formation rate constants for both phen and bipy are much smaller than the corresponding calculated rate constants as shown in Table 14. This could be accounted for by either a shift in the RDS from initial bond formation to ring closure or by severe steric hindrance which affects initial bond formation. The shift of RDS from the point of the first bond formation

to that of the ring closing step for highly substituted ligands which impose steric hindrance in formation reaction had been suggested by many people.[13,17-20]

The reaction of NH_3 with hexaaquo nickel gives a k_f value of 4.3×10^3 $M^{-1}sec^{-1}$ while that for phen and bipy give 3.9×10^3 $M^{-1}sec^{-1}$ and 1.61×10^3 $M^{-1}sec^{-1}$ respectively. Clearly ring closure here does not limit the observed formation rate in the case of phen. This is also true in the reactions of Ni(II) and unsubstituted polyamines.[1,33,34] The location of RDS[35] depends on the ratio of k_{23}/k_{21}. It can be shown that the ratio k_{23}/k_{21} has a value of 0.5 for bipy reacting with Ni(II) and 1.5 for phen reacting with Ni(II). The values of these ratios are obtained by calculating k_{23} from equation 20a using the dissociation rate of nickel pyridine as k_{21} and known values of k_f, K_{os}, and k_{12}. Thus ring closure contributes to the limiting rate in the case of bipy but not in phen.

The reason for this difference may be in the fact that bipy has rotational freedom between the two heterocyclic rings but phen does not. This freedom, as shown in the structure formula in Fig. 25, makes a bipy molecule more flexible than a rigid phen and allows it to adapt a more stable conformation than phen. The dipole moment of pyridine is 2.19 debye.[36] This rather large

dipole moment may cause the two pyridine rings of bipy to rotate to have a trans conformation as shown below.

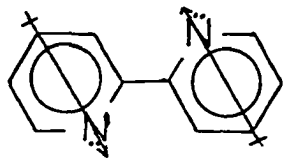

If this is true and since the two dentate sites of phen and bipy have to be on a plane (cis conformation with respect to N dentate sites of the ligands) for coordination to $Ni(trien)^{2+}$, phen which already is on a plane to coordinate to $Ni(trien)^{2+}$ would coordinate at a faster rate than bipy. The reactions of bipy may be termed conformationally controlled substitution reactions. The rotational freedom of bipy then hinders the cis conformation requirement to coordinate. This is also true without the consideration of dipole moment.

The factor of about two seen between k_f for phen and k_f for bipy reacting with Ni(II) is repeated as ligands are added to the metal ion. If the RDS shifts from first bond formation to ring closure as nickel(II) is coordinated with more highly substituted polyamine, then it would be shown in the ratio k_f, phen/k_f, bipy because the conformational effect of bipy must become more pronounced as nickel(II) is coordinated with more highly substituted polyamine. However, the ratio k_f,phen/k_f, bipy is 2.4 for $Ni(H_2O)_6^{2+}$, 1.9 for $Ni(en)^{2+}$,

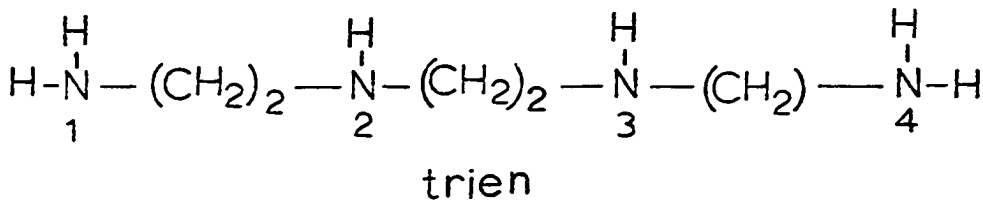

trien

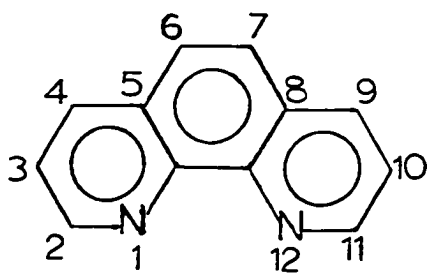

phen

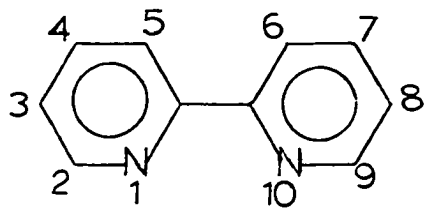

bipy

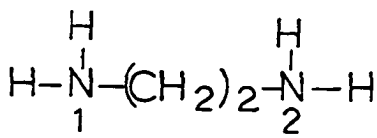

en

Figure 25. Structure Formulas of some of Ligands Used

2.1 for $Ni(dien)^{2+}$, 1.1 for $Ni(en)_2^{2+}$, 3.6 for $Ni(trien)^{2+}$ and 1.3 for Ni(tren). (See Table 14.) The reasonably constant value of these ratios indicates that the k_{23}/k_{21} ratio for phen and bipy reacting with the above mentioned nickel complexes must stay about the same. Thus initial bond formation is still the major rate limiting factor for phen and bipy reacting with the severely hindered $Ni(trien)^{2+}$ and $Ni(tren)^{2+}$ complexes. This means that the decrease in k_f seen for phen and bipy reacting with $Ni(en)^{2+}$, $Ni(en)_2^{2+}$, $Ni(dien)^{2+}$, $Ni(trien)^{2+}$ and Ni(tren) must be a steric factor involved in initial bond formation.

Previous studies on other nickel-ligand formation rates attributed a decrease in the formation rate constant to steric effects.[25,26,37,38] To facilitate correlation of the values of the formation rate constants to steric effects, an organic substituent function, E_s, can be calculated[37] using the formula,

$$E_s = \log \left(\frac{k_{obsd}}{k_{ref}} \right) \qquad (25)$$

Where k_{ref} is a reference rate constant equal to $K_{os}k^{-H_2O}$. Values of E_s for phen and bipy were calculated and are listed in Table 14. A general trend is seen in the E_s values of phen reacting with various

Ni(II) complexes. As the coordination sphere of Ni(II) gets filled, E_s becomes more negative indicating a larger steric effect. The same is seen for bipy after correcting the observed rate constant for the ring closure contribution using a factor of 2. This steric effect may be caused by the hydrogen-hydrogen repulsion between hydrogens on the No. 1 and 4 nitrogens of trien (see Fig. 25) and those on the No. 2 and 11 carbons of phen (No. 2 and 9 carbons for bipy).

Triethylenetetramine Nickel(II) With Ethylenediamine and n-Propylamine

The complicated anomalous transmittance changes observed during the reaction of en and $prNH_2$ with $Ni(trien)^{2+}$ were also reported by Rorabacher and co-workers[39] in their study of the kinetics of aquonickel(II) ion reacting with en. Explanation for the anomaly is not given.

The calculated formation rate constant for both etylenediamine and propylamine reacting with $Ni(trien)^{2+}$ is 2.7×10^5 $M^{-1}sec^{-1}$ which exceeds the upper limit of detectability of the stopped-flow spectrophotometer. The experimental formation constant for the $Ni(trien)^{2+}$-NH_3[10] system at 8^oC is 1.2×10^5 $M^{-1}sec^{-1}$. At 25^oC, this would be a little larger, probably close to the calculated value of 2.7×10^5 $M^{-1}sec^{-1}$. The formation rate

constant for $Ni(trien)^{2+}$-$prNH_2$ and $Ni(trien)^{2+}$-en systems may be a little smaller than that for $Ni(trien)^{2+}$ -NH_3 due to steric effects of the N-ethyl and propyl group on the bonding nitrogen[38] but still would be above the upper limit of detectability using the stopped-flow spectrophotometer. Margerum and Jones[13] in their study of the equilibrium between $Ni(en)_2^{2+}$ and $Ni(en)_3^{2+}$ reported that the rate of the first bond formation for the reaction between $Ni(en)_2$ and en is 5.5×10^6 $M^{-1}sec^{-1}$ and that of the ring closure is 2.2×10^5 sec^{-1}. This system comes very close to approximating $Ni(trien)^{2+}$-en system. The $Ni(en)_2^{2+}$-en system also provides data to show that there is no steric effect in the reaction of $Ni(en)_2^{2+}$ and en. The value of initial bond formation for $Ni(H_2O)_6^{2+}$ and Hen^+ is calculated to be 4.8×10^2 $M^{-1}sec^{-1}$ using eq. 2 with $K_{os} = 0.018$ M^{-1} (eq. 22) and $k^{-H_2O} = 2.8 \times 10^4$ sec^{-1}.[32] The corresponding value for $Ni(en)_2$ and Hen^+ is 9.7×10^4 $M^{-1}sec^{-1}$ using k^{-H_2O} $= 5.4 \times 10^6 sec^{-1}$ (Table 14). The use of Hen^+ eliminates the internal conjugate base (ICB) effect from accelerating the formation rate. The experimental values for $Ni(H_2O)_6^{2+}$ and $Ni(en)_2^{2+}$ reacting with Hen^+ are 5.9×10^2 $M^{-1}sec^{-1}$ [40] and 1.1×10^5 $M^{-1}sec^{-1}$ [13] respectively and show the same ratio as the rate of water loss values do. Thus no steric effect is present. Similar reasoning

cannot be used for $Ni(H_2O)_6^{2+}$ reacting with en because the effect of the coordinated en molecules on the ICB effect is not known. This also means that the bulk of the aromatic rings in phen and bipy account for the large deviation of experimental formation rate constants from the calculated rate constant as seen in their reactions with $Ni(trien)^{2+}$.

Triethylenetetramine Nickel(II) With Glycine And 2-Pyridinecarboxylic Acid

Glycine and 2-pyridinecarboxylic acid exist as dipolar ions (zwitter ion) in neutral solution and as a completely unprotonated ion at a higher pH as shown for glycine in eq. 26.

$$H_2NCH_2COO^- \underset{}{\overset{OH^-}{\rightleftharpoons}} H_3\overset{+}{N}CH_2COO^- \overset{H^+}{\rightleftharpoons} H_3\overset{+}{N}CH_2COOH \qquad (26)$$

Two bonding sites exist in unprotonated gly and pyc, the amino group and the carboxylate group.

Recently Margerum et. al.[12] established, with experimental evidence, the reason why the carboxylate group must bond first, followed by ring closure involving the amino group. Jordan and Letter[41] have also presented evidence showing that initial bond formation involves the carboxylate group in amino acids and amino carboxylates. They further showed that the zwitter ion can be a reactive species, contrary to previous work.[40]

As stated in Chapter IV, and equilibrium shift between the intermediate species A and B in Fig. 26 is the cause of the absorbance change as a function of pH in 1:1 $Ni(trien)^{2+}$-gly solutions. These species are formed rapidly, as evidenced by the zero-order behavior seen for gly and pyc. The rate constants (Table 11) obtained from first-order rate plots of second-order (1:1 $Ni(trien)^{2+}$ and gly) kinetic runs at pH 8.3 for gly and at pH 8.8 for pyc give much lower values than those from runs made under pseudo first-order conditions with a 10-fold excess of gly at the corresponding pH's. This is due to incomplete formation of the $Ni(trien)\text{-}gly^{+}$ intermediate from the $Ni(trien)\text{-}glyH^{2+}$ species at lower pH as shown in Fig. 26 (intermediate A goes to B). Thus, in a 1:1 solution of $Ni(trien)^{2+}$ and glycine, there are appreciable amounts of both A and B at equilibrium and changes in pH cause a shift in the equilibrium $A \rightleftharpoons B$. This shift is seen as an absorbance increase as A goes to B. The value of K_a for $A \longrightarrow B$ may be obtained from the inflection point of the absorbance vs pH plot (Fig. 12)

It is evident from the experimental results of this study that the observed reaction is intramolecular, that is, the observed reaction involes the ring closing

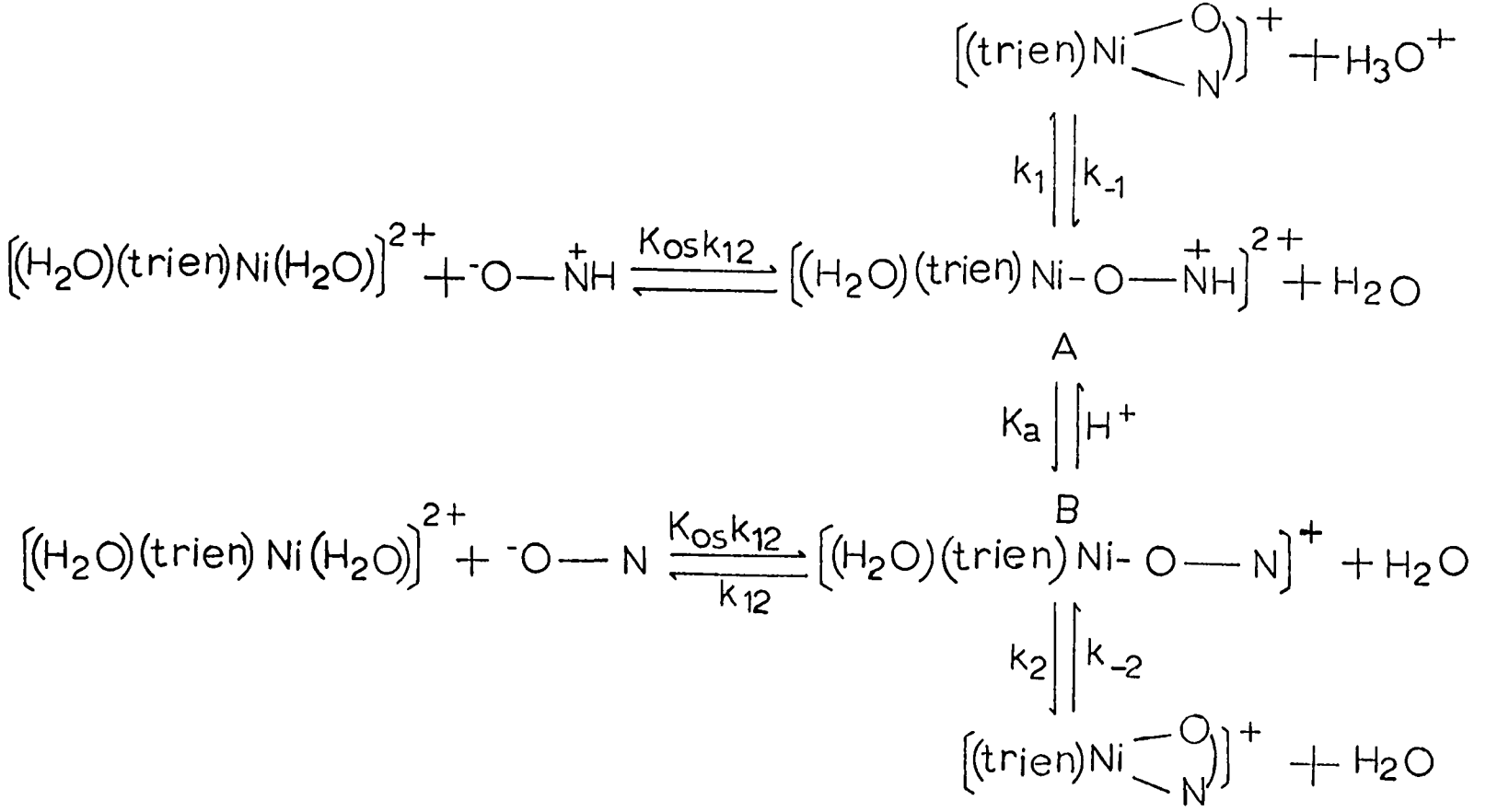

Figure 26. Proposed Mechanism of the Reaction of Glycine and 2-Pyridinecarboxylic Acid with Triethylenetetramine Nickel(II)

step only. This was shown by zero-order kinetic behavior in ligands. Thus the observed rate constants at higher pH correspond to k_2 in Fig. 26. Since at a lower pH k_1 dominates and at higher pH k_2 dominates for both gly and pyc, resolution of the formation constants (see eqs. 17 and 18) require the values of K_a, the acid dissociation constants of species A in Fig. 26. These values were estimated as described in Chapter IV for both Ni(trien)-glyH^{2+} and Ni(trien)-pycH^{2+}. The pK_a values for free gly$^-$ and free pyc$^-$ are listed in Table 15. The corresponding K_a values for the carboxylate group bonded species are also listed in Table 15. For gly, the bound K_a is approximately 100 times greater than free K_a. Taube and co-workers[42] have shown that for gly bonded to $(NH_3)_5Co^{3+}$ at μ = 0.03 M, the K_a value of the $-NH_3^+$ group is about twenty times greater than that for the free gly zwitter ion. In their study, however, the $-NH_3^+$ group is deprotonated but does not coordinate to the metal. No explanation is available for the increase in K_a seen in the protonated Ni(trien)-gly^{2+} intermediate or lack of any increase seen for protonated Ni(trien)-pyc^{2+} intermediate.

Wilkins et. al.[40] have suggested that the zwitter ion form of amino acids and aminocarboxylates is extremely unreactive. Jordan and Letter[41] and Margerum[49] refuted this. The data (Table 12) obtained in this

TABLE 15

K_a Values of Glycine And Pyridinecarboxylate

Ligand	Free K_a[a], M	Bound K_a[b], M
gly^-	2.69×10^{-10}	3.16×10^{-8}
pyc^-	6.2×10^{-6}	3.2×10^{-6}

a. Values cited from A. E. Martell and R. M. Smith, "Critical Stability Constant," 1947 and is expressed as $\frac{[^-O\text{-}N][H^+]}{[^-O\text{-}NH^+]}$

b. Estimated in this study and is expressed as $\frac{[TNi\text{-}O\text{-}N][H^+]}{[TNi\text{-}O\text{-}NH]}$ where T is trien and charges are omitted for the sake of convenience.

study show that the zwitter ion forms of glycine and pyc are reactive. The k_2 values for gly and pyc show that ring closure involving the $-NH_2$ is approximately 1.2 times greater than that involving the  . The k_1 values for gly and pyc, however, show protonated aromatic nitrogen () ring closure to be about three times larger than that for protonated aliphatic nitrogen ($-NH_3^+$). These k_1 values represent reactivity of the zwitter ion.

The effect of trien sterically hindering ring closure may be seen by comparing k_2 for $Ni(trien)(gly)^+$ with the calculated value of ring closure for $Ni(gly)^+$ formation. Using $K_{os} = 1.92\ M^{-1}$, $k^{-H_2O} = 2.8 \times 10^4 sec^{-1}$, $k_f = 2.2 \times 10^4\ M^{-1}sec^{-1}$ (see Table 14), $k_{21} = 5 \times 10^3\ sec^{-1}$ [50] and eq. 20a, the value of k_{23} in eq. 19c is calculated to be $2 \times 10^3 sec^{-1}$. This agrees well with an estimated value[51] of $1 \times 10^3 sec^{-1}$. The k_2 values obtained from the present study are about 10^2 thus E_s values would be about -1 using the calculated value as the reference.

The actual values are shown in Table 14. The difference between k_1 and k_2 for the same ligand represents ring closure involving an unprotonated dentate site compared to a protonated one. The ratios k_2/k_1 of gly and pyc are 13 and 3.4 respectively. The

difference between the two rate constants, k_1 and k_2 cannot be due to a change in rate of water loss since the same groups are coordinated to Ni(II) regardless of whether the nitrogen is protonated or not. It can, however, be attributed to a sluggish rate of proton transfer from $[Ni(trien)-O-\overset{+}{N}H]^{2+}$ to water. The proton transfer is relatively slow[52,53] and has been estimated as $10^2 sec^{-1}$ for $M-OOCCHRNH_3^+$ and measured as $3.16 \times 10^2 sec^{-1}$ at 37°C for Cu (serine H)$^+$.[54] The same factor of about 10 between ring closure for gly reacting with unhindered nickel(II) and with $Ni(trien)^{2+}$ is seen in the comparison between expected ring closure values of about $10^2 sec^{-1}$ and the observed ring closure values of gly and pyc reacting with $Ni(trien)^{2+}$ of about 10-20 sec^{-1}. This is not unexpected since after the proton is lost, the steric effects in the k_1 and k_2 pathways are identical. The E_s values for gly and pyc are shown in Table 14 using $10^2 sec^{-1}$ as the reference value. The difference between E_s values of the protonated gly and protonated pyc can be explained by proximity effects which have been shown to be important in ring closure reactions.[55] For example, six-membered ring closure compared with five-membered ring closure can be up to 8 times slower due to proximity effects. The aliphatic zwitter ion has three protons on the nitrogen donor

atom compared to only one for the aromatic zwitter ion. Thus hydrogen bonding to three water molecules is possible for glycine but only to one water molecule for pyc. This will cause the nitrogen dentate site of glycine to be farther away from the nickel coordination site than the aromatic nitrogen of pyc and, as the proximity effects seen in five- and six-membered rings, will reduce the ring closure rate.

REFERENCES

1. R. G. Wilkins and M. Z. Eigen, "Mechanisms of Inorganic Reaction," 49(1965), pp. 55-f

2. T. R. Stengle and C. H. Langford, Coord. Chem. Rev. 2, 349(1967)

3. J. Swinehart and K. Kustin, Prog. Inorg. Chem., 13 (1970)

4. J. P. Hunt, Coord. Chem. Rev. 7, 1(1971)

5. T. J. Swift and R. E. Connick, J. Chem. Phys. 37, 307(1962)

6. R. G. Wilkins, Accounts Chem. Res. 3, 408(1970)

7. R. M. Fuoss, J. Am. Chem. Soc. 80, 5059(1958)

8. M. Z. Eigen, Phys. Chem., NFI, 176(1954)

9. D. W. Margerum and H. M. Rosen, J. Am. Chem. Soc. 89, 1088(1967)

10. D. W. Margerum, J. P. Jones and E. J. Billo, J. Am. Chem. Soc. 92, 1875(1970)

11. G. Gordon, W. Melvin and D. P. Rablen, Inorg. Chem. 11, 488(1972)

12. A. E. Martell (ed.), "Coordination Chemistry," 2, (1978), pp. 42-f.

13. J. P. Jones and D. W. Margerum, J. Am. Chem. Soc. 92, 470(1970)

14 F. P. Cavasino, E. DiDio and G. Calvarvso, J. Chem. Soc., Dalton Trans.,1972, 2632

15. F. P. Cavasino, E. DiDio and G. Locanto, J. Chem. Soc., Dalton Trans., 1973, 2619

16. G. Calvarvso, E. DiDio and F. P. Cavasino, J. Inorg. Nucl. Chem. 36, 2061(1974)

17. K. R. Kustin, R. R. Pasternack and E. M. Weinstock, J. Am. Chem. Soc. 88, 4610(1966)

18. A. Kowalak, K. Kustin, R. F. Pasternack and S. Petrucci, J. Am. Chem. Soc. 89, 3126(1967)

19. K. Kustin and R. F. Pasternack, J. Am. Chem. Soc. 90, 2295(1968)

20. R. F. Pasternack and K. Kustin, J. Am. Chem. Soc. 90, 2805(1968)

21. J. C. Cassatt, R. F. Pasternack and E. Gibbs, J. Phys. Chem. 73, 3814(1969)

22. R. Reingold, L. Gipp, M. Angwin and R. F. Pasternack, J. Am. Chem. Soc. 91, 4083(1963)

23. D. B. Rorabacher and C. Lin, Inorg. Chem. 12, 2420 (1973)

24. A. E. Martell, ibid., pp. 38

25. D. B. Rorabacher and T. S. Turan, Inorg. Chem. 11, 288(1972)

26. T. S. Turan, Inorg. Chem. 13, 1584(1974)

27. J. S. Fritz, J. E. Abink and M. A. Payne, Anal. Chem. 33, 1381(1961)

28. C. N. Reilley, Chemist-Analysts, 46 (No. 3); 59(1957)

29. G. G. Hammes and J. I. Steinfeld, J. Am. Chem. Soc. 84, 4639(1962)

30. G. G. Hammes and M. L. Morrell, ibid., 86 1497(1964)

31. G. H. Nancollas and N. Sutin, Inorg. Chem. 3, 360 (1964)

32. A. E. Martell, ibid., p. 133

33. D. W. Margerum, D. B. Rorabacher and J. F. G. Clarke, Jr., Inorg. Chem. 2, 667(1963)

34. R. H. Holyer, C. D. Hubbard, S.F.A. Kettle and R. G. Wilkins, Inorg. Chem. 4, 929(1965)

35. A. E. Martell, ibid., p. 35

36. R. C. Weast, "Handbook of Chemistry and Physics," 52nd edition, 1971, pp. E-53

37. D. B. Rorabacher, T. S. Turan, J. A. Defever and W. G. Nickels, Inorg. Chem. 8, 1498(1969)

38. D. B. Rorabacher and C. A. Melendez-Cepeda, J. Am. Chem. Soc., 93, 6091(1971)

39. R. W. Taylor, H. K. Stepien and D. B. Rorabacher, Inorg. Chem. 13, 1282(1974)

40. J. C. Cassatt and R. G. Wilkins, J. Am. Chem. Soc. 90 6045(1968)

41. R. B. Jordan and J. E. Letter, J. Am. Chem. Soc. 97, 2381(1975)

42. R. Holweda, E. Deutsch and H. Taube, Inorg. Chem. 11, 1965(1972)

43. K. Kustin and J. Swinehart, Prog. Inorg. Chem. 13, 107(1970)

44. P. K. Chattopadhyay and J. F. Coetzee, Inorg. Chem. 12, 113(1973)

45. R. W. Taylor, D. B. Rorabacher and H. K. Stepien, Inorg. Chem. 13, 1282(1974)

46. D. B. Rorabacher, Inorg. Chem. 5, 1891(1966)

47. J. C. Cassatt and R. G. Wilkins, J. Am. Chem. Soc. 90, 6045(1968)

48. J. C. Cassatt, W. A. Johnson, L. M. Smith and R. G. Wilkins, ibid., 94, 8399(1972)

49. A. E. Martell, ibid., p. 59

50. loc. cit., p. 39

51. loc. cit., p. 61

52. M. Eigen, Angew. Chem. Int. Ed. Engl., 3, 1(1964)

53. M. Eigen, G. Kruse, G. Maass and L. DeMaeyer, Pro. React. Kinet., 2, 287(1964)

54. V. S. Sharma and D. L. Leussing, Inorg. Chem. 11, 138(1972)

55. A. E. Martell, ibid., p. 37

APPENDIX

The relationship between concentration of $Ni(trien)^{2+}$ and absorbance needed for a second-order plot having equal concentration of reactants as shown in Fig. 15 for phenanthroline is derived with A_t representing absorbance at any time, A_f representing the final absorbance and C^o representing the initial concentration. Charges on reactants are omitted for clarity and trien and phen are further abbreviated to T and P respectively. The value of molar absorptivities of reactants and product are known from the spectra of each solution. Assuming Beers law to hold, the absorbance at any time is equal to the absorbance of the reactants left and the product formed. Then, at λ = 343 nm

$$\epsilon_{NiT} \ll \epsilon_p$$

$$C_{NiT} = C^o_{NiT} - C_{NiTP} \qquad (1a)$$

$$C_{NiTP} = C^o_{NiT} - C_{NiT} \qquad (1b)$$

$$C_p = C^o_{NiT} - C_{NiTP} \qquad (1c)$$

$$A_f = \epsilon_{NiTP} C^o_{NiT} \qquad (2)$$

$$A_f = \epsilon_{NiTP} C_{NiTP} + \epsilon_p C_p \qquad (3a)$$

Substituting eqs. 1b and 1c into eq. 3a,

$$A_t = \epsilon_{NiTP}(C^o_{NiT} - C_{NiT}) + \epsilon_p\{C^o_{NiT} - (C^o_{NiT} - C_{NiT})\} \qquad (3b)$$

Substituting eq. 2 into eq. 3b,

$$A_t = A_f - (\epsilon_{NiTP} - \epsilon_p)\, C_{NiT} \qquad (4)$$

Hence $$\frac{1}{C_{NiT}} = \frac{\epsilon_{NiTP} - \epsilon_p}{A_f - A_t} \qquad (5)$$

The concentration-absorbance relationship for second-order plots having equal concentration of reactants for both glycine and 2-pyridinecarboxylic acid are derived in a manner similar to that for phenanthroline.

For glycine at λ = 260 nm,

$$\frac{1}{C_{NiT}} = \frac{\epsilon_{NiTG} - \epsilon_{NiT}}{A_f - A_t} \qquad (6)$$

where G is glycine.

For 2-pyridinecarboxylic acid at λ = 234 nm where $\epsilon_{NiT} = \epsilon_{pyc}$,

$$\frac{1}{C_{NiT}} = \frac{\epsilon_{NiTpyc} - 2\epsilon_{NiT}}{A_f - A_t} \qquad (7)$$